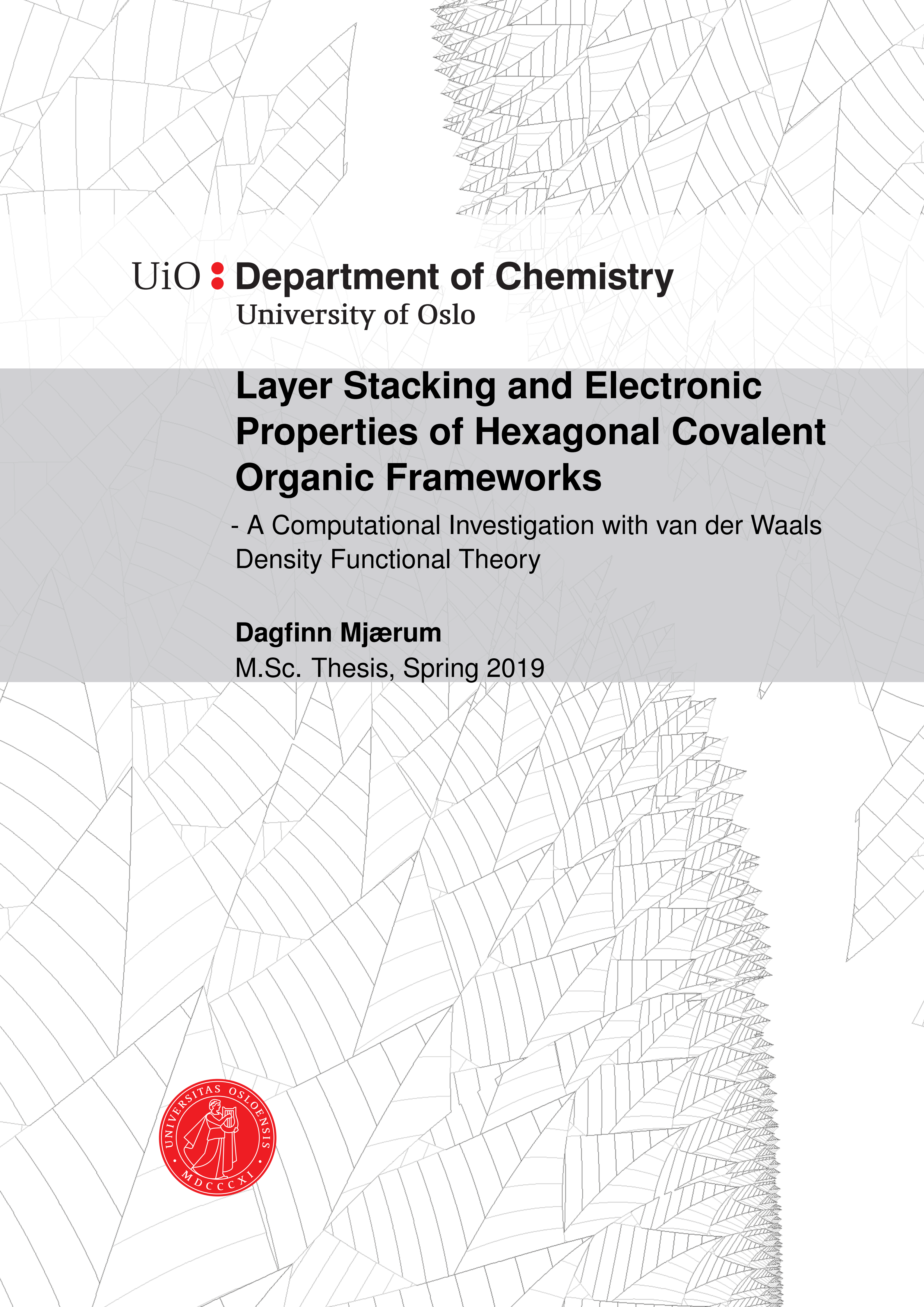

UiO : **Department of Chemistry**
University of Oslo

Layer Stacking and Electronic Properties of Hexagonal Covalent Organic Frameworks

- A Computational Investigation with van der Waals Density Functional Theory

Dagfinn Mjærum
M.Sc. Thesis, Spring 2019

LAYER STACKING AND ELECTRONIC PROPERTIES OF HEXAGONAL COVALENT ORGANIC FRAMEWORKS

—

A COMPUTATIONAL INVESTIGATION WITH VAN DER WAALS DENSITY FUNCTIONAL THEORY

DAGFINN MJÆRUM

UiO : University of Oslo

M.SC. THESIS IN MATERIALS, ENERGY AND NANOTECHNOLOGY

DEPARTMENT OF CHEMISTRY

UNIVERSITY OF OSLO

MAY 2019

SUPERVISORS:
PROF. CLAS PERSSON,
ASSOCIATE PROF. KRISTIAN BERLAND
& ADJUNCT PROF. OLE MARTIN LØVVIK

© DAGFINN MJÆRUM

2019

Layer Stacking and Electronic Properties of Hexagonal Covalent Organic Frameworks

Dagfinn Mjærum

https://www.duo.uio.no/

Print: Reprosentralen, University of Oslo

Abstract

We have calculated the electronic properties and layer stacking patterns for a group of twelve hexagonal covalent organic frameworks. This has been done in order to explore this group of materials on a fundamental level and aim to lay the ground work for further studies, which will focus on assessing these frameworks as useful materials for electronic and optoelectronic devices. To explore these materials, we have deployed numerical density functional theory calculations. A Van der Waals density functional is used to describe non-local correlation effects that give rise to stabilizing van der Waals forces, essential in layered systems. We found that all the materials prefer to stack in specific configurations close to AA-stacking, where subsequent layers are placed directly on-top of each other. We also found that the materials exhibit dispersion in the out-of-plane direction when we go from two-dimensional single layers to three-dimensional stacks.

Abbreviations

Abbreviation used in the thesis:

ACF = Adiabatic Connection Formula
BDBA = Benzenediboronic Acid
BET = Brunauer–Emmett–Teller
BS = Band Structure
CBM = Conduction Band Minimum
COF = Covalent Organic Framework
CTF = Covalent Triazine Framework
cx = consistent exchange
DFT = Density Functional Theory
GGA = Generalized Gradient Approximation
DOS = Density of States
HHTP = hexahydroxytriphenylene
KS = Kohn-Sham
MOF = Metal Organic Framework
PBE = erdew-Burke-Ernzerhof
POF = Porous Organic Framework
PPy = Polypyrene
TP = Triphenylene
UC = Unit Cell
vdW = Van der Waals VBM = Valence Band Maximum
vdW = van der Waals
XC = Exchange Correlation

Contents

Abstract iii

Abbreviations v

Acknowledgements ix

1 Introduction 1
1.1 Covalent Organic Frameworks 1

2 Theory 5
2.1 Quantum Mechanical Modeling - DFT 5
2.2 Kohn-Sham Equations 5
2.3 Different Functionals 7
2.4 Band Structure and Density of States 8

3 Methodology 9
3.1 Relaxation 9
3.2 Convergence Testing 10
3.3 Band Structure and Density of States 11
3.4 Stacking 12
3.5 Precursor Calculations 13

4 Results 15
4.1 Total Energy and Stability 15
4.2 Crystal Structure 16
4.3 Band Structure and Density of States 16
4.4 Stacking Study 22

5 Conclusions 27
5.1 Electronic Properties 27
5.2 Stacking 27
5.3 Stability 28

Bibliography 30

Appendices 31

A Appendix 1 **33**
A.1 Single Layer BS and DOS 33
A.2 Layered BS and DOS 38

List of figures **47**

List of tables **49**

Acknowledgements

I would like to take this opportunity to thank all the people that helped me write this thesis. First of all I would like to thank my supervisors Clas Persson, Kristian Berland and Ole Martin Løvvik for your help, guidance, and motivation. Then I would like to thank the rest of the members of my research group for helpful discussions and great memories. The extended network at the Centre for Materials Science and Nanotechnology also deserve gratitude, in particular Christian Fleischer for providing me with the LaTeX template for this document. I will also like to thank NOTUR for granting me access to HPC resources, which enabled me to preform my calculations. At last I will like to thank my family, my friends and my partner Karolina Eriksen for patience and support throughout this process.

1

Introduction

1.1 Covalent Organic Frameworks

Covalent organic frameworks (COFs) are man-made materials, synthesized through ordered polymerization of organic monomers. They form gird-like crystalline structures in two or three dimensions. The structures are characterized by their nanometer-sized voids or channels through the material. COFs consist only of the light main group elements (H, B, C, N and O) that are known to form strong covalent bonds. Due to this fact COFs are typically more chemically robust compared to related framework structures like metal-organic frameworks[1], which in addition incorporates metal ions or clusters into the organic framework.

Imagine the bonding in a sheet of graphene. Atoms are arranged periodically in a honeycomb-like pattern with carbon atoms in the corner of each symmetry-equivalent hexagon. Imagine increasing the size of this pattern by one order of magnitude. Switch every carbon atom with small organic units with three fold rotational symmetry and replace the carbon-carbon bonds with short polymers with two fold rotational symmetry. Now the space within each hexagon, which previously was occupied with electron density from the carbon π-orbitals, is open and can fit different molecules or ions. This is the general form of the 2D hexagonal COFs that will be discussed in this thesis (see Figures 1.1 and 1.2).

To explore this material class we deploy numerical density functional theory. A computational quantum mechanical modeling method based on Schrödinger-like equations. This method uses a few different approximation, which will be discussed in the theory part, to solve quantum mechanical systems far too complicated to be evaluated analytically. With this approach we are able to investigate properties of theoretically proposed or experimentally realized materials. It is a versatile tool that can help in every stage of a material or component development process. It can work as a screening process, to map the landscape of possible candidate materials before efforts are made to synthesize the most promising candidates or it can be used in tight collaboration with experimental work, aiding in understanding and explaining results. In this thesis DFT is mainly used in the first way, as a screening tool candidate materials. When theory and experimental measurements agree they strengthen each other but when they deviate we can discover errors or flaws in our reasoning, which may lead to greater overall understanding.

Can we understand the effects of structural or compositional changes in frameworks with the

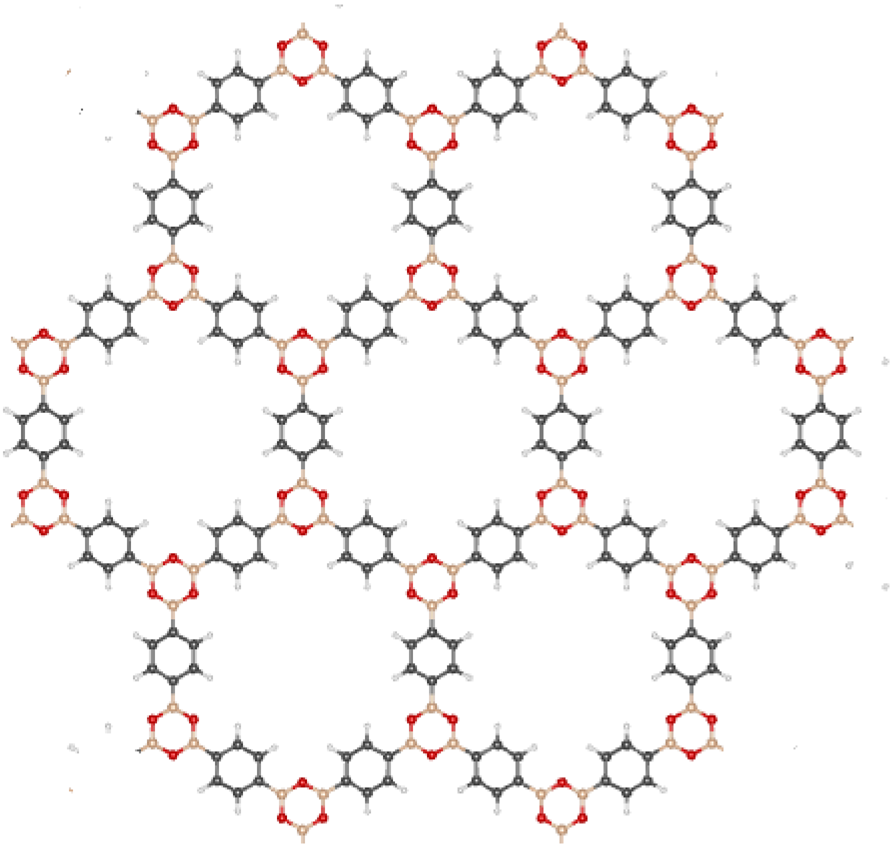

Figure 1.1: Illustational picture of a single layer of COF-1. Boron, oxygen, carbon and hydrogen are represented with pink, red, black and white, respectively. Twelve hexagonal boroxide and phenyl rings combine to construct bigger hexagonal pores. The boroxide rings have three fold rotational symmetry and are referred to as nodes while the phenyl rings with two fold rotational symmetry and are referred to as linker.

same underlying structure? This will enable us to predict or provoke material behavior. DFT calculations are perfect for this task as they give a quantitative comparison of different variations of these materials. As an example, one has the ability to choose to model the material with different crystal structures or in otherwise different configuration, without all of them necessarily being chemically or thermodynamically viable options. In reality, only the most stable of your configurations, if any, have the chance to appear if there are big differences in total energy between different structural configurations of the material. It enables us to compare and see trends that are not possible in the laboratory. This is important in terms of COFs because of the sheer amount of possible candidate materials available. The freedom of organic chemistry cross paths with the control of solid-state physics when a diverse selection of molecular building blocks can crystallize into extended frameworks. High chemical and thermodynamic stability caused by strong covalent bonds enables them to retain their geometry when foreign chemical species are incorporated into the pores[1]. This opens up a wide range off possibilities for combining different species inside the well defined structures. This is a dream come true for material scientists.

Framework materials like COFs and the more famous metal-organic frameworks (MOFs) have mainly been investigated for their promising porous properties. The large regularly spaced

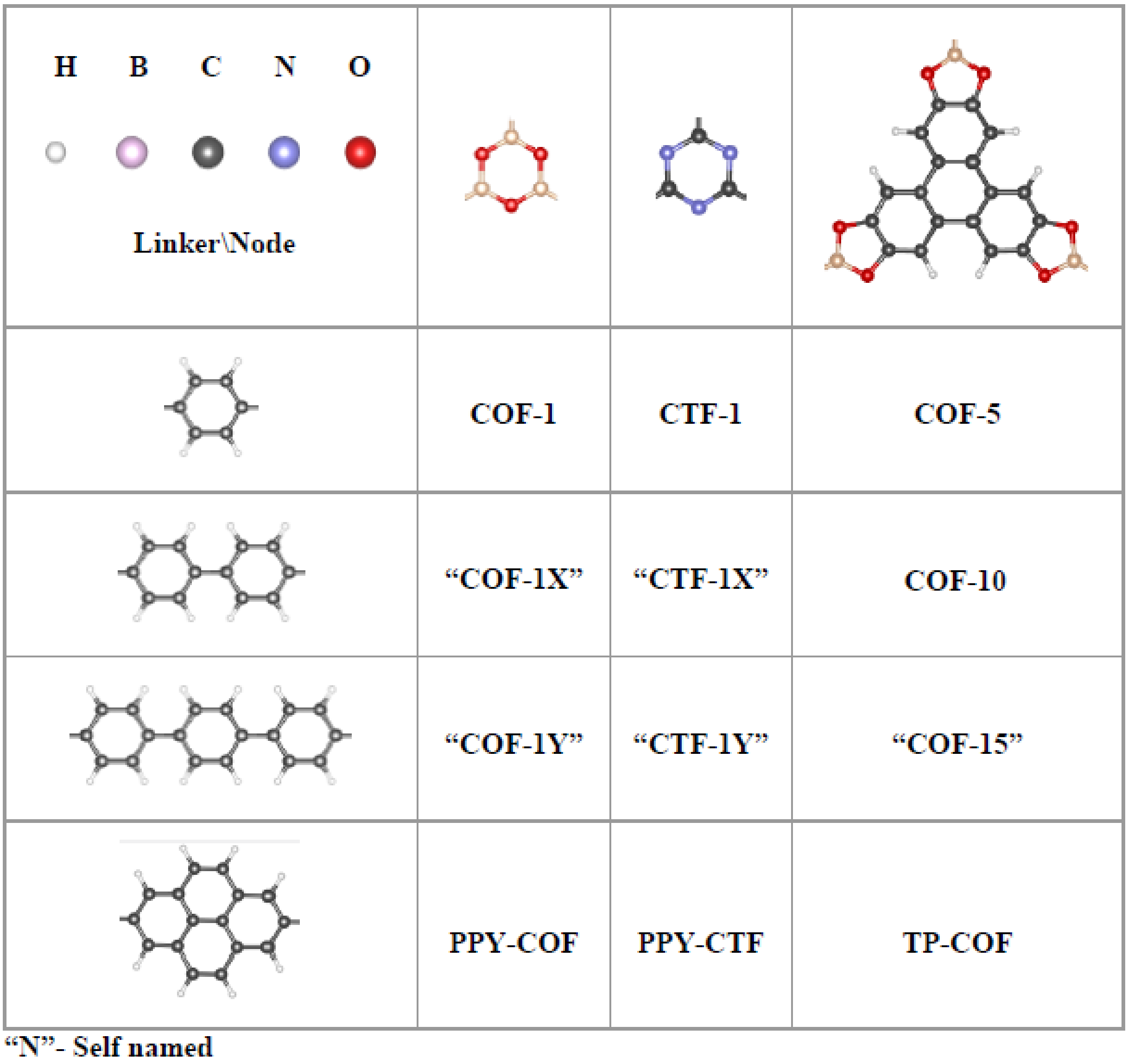

H B C N O ○ ● ● ● ● Linker\Node			
	COF-1	CTF-1	COF-5
	“COF-1X”	“CTF-1X”	COF-10
	“COF-1Y”	“CTF-1Y”	“COF-15”
	PPY-COF	PPY-CTF	TP-COF

“N”- Self named

Figure 1.2: In the diagram we see the different possible combinations of linkers and nodes that make up our candidate materials. These are not the chemical precursors but just the molecular building units (with dangling bonds) we can imagine combining to form the extended structures.

pores of MOFs have scored many new records regarding BET surface area[2]. Recent theoretical works have also suggested interesting electronic properties[3][4][5]. In this study we have calculated band structure and density of states for a group of twelve COFs, which all share a similar hexagonal structure with atoms played in a honeycomb-like pattern. Both as isolated single layers and as Stacked structures. The candidate materials can be seen in figure 1.2 and result from all possible combinations of four linkers and three nodes. This work will lay the foundation for a further study into the field, which will aim to identify COFs that can be tailoring into usable components for electronic and optoelectronic devices.

Our simplest COFs in terms of size and number of electrons are COF-1 and CTF-1 (T = Triazine) (see Figures 1.2 and 1.1). They have the smallest integer elemental compositions BC_3H_2O and C_4H_2N, respectively. They are structurally equivalent, but the boron atoms are switched with carbon and the oxygen atoms are replaced with nitrogen when we go from COF-1 to CTF-1. Single layers structures of both materials have a relatively small unit cells (UC), containing 42 atoms and 138 valance electrons. This reduces computational time significantly compared to the larger COFs. For this reason these materials have preferably been used for method testing and test studies. COF-1 is build up by hexagonal boroxine and phenyl rings which in turn forms bigger hexagonal frameworks. Three-armed boroxine rings work as “nodes” in the corners of each big hexagon and the two-armed phenyl rings are used as “linkers” between the nodes. COF-1 and CTF-1 have intuitively simple net reaction pathways as only one precursor molecule is needed. For COF-1 1,4-benzenediboronic acid (BDBA) reacts with itself in a condensation reaction, releasing water. A realistic reaction mechanism is more complicated as it involves intermediates assisted by catalysts[1] but the net reaction which creates one UC of COF-1 can be seen in Equation 1.1 bellow. The aggregation states are not specified as different synthesis methods exist.

$$3\ B_2C_6H_8O_4 \rightarrow B_6C_{18}H_{12}O_6 + 6\ H_2O \tag{1.1}$$

We can imagine the larger frameworks to have similar reaction pathways, but these will generally not have a single organic monomer as reactant, but rather two different reactants condensing into a framework, complicating synthesis.

In addition to COF-1 and CTF-1 this research is extended to similar larger structures, both in terms of number of atoms in the UC and pore diameter. Ten larger structures have also been considered. Four of them are very similar, with just the addition of one or two extra phenyl rings on the linker of COF-1 and CTF-1, we call these COF-1X, COF-1Y, CTF-1X and CTF-1Y. PPy-COF and PPy-CTF have the same nodes as COF-1 and CTF-1, respectively, but use linkers based on flat aromatic pyrene molecules. The four remaining COFs all share a common node unit based on the hexahydroxytriphenylene (HHTP) molecule but differ in their choice of linker as they arise from combination of all linkers mentioned above. With the same linkers as COF-1, COF-1X, COF-1Y and PPy-COF we have COF-5, COF-10, COF-15 and TP-COF (Triphenylene), respectively. By choosing similar structures we discover common trends and deviations from them that can help us forge a fundamental understanding of these new framework materials.

2

Theory

2.1 Quantum Mechanical Modeling - DFT

Density functional theory is a computational modeling method used to investigate the electronic structures of the ground state in many-body systems like atoms or molecules. The theory is formulated in such a way that properties of the system can be determined by looking at the spatial electron density functional, hence the name. The theory is formally exact for the ground state but the exact form is not known. So in practice one relies on an approximate treatment of the most computationally demanding terms in the equations. This approximate treatment can reduce a complicated many-body system into single-particle equations that can be solved independently. When modeling the system this can reduce computational time by orders of magnitude compared to more exact methods, allowing the study of more and larger systems.

The results were constructed using numerical density functional theory calculations within the Vienna Ab initio Simulation Package (VASP). VASP is a plane-wave code which uses periodic boundary conditions. This allows for the modeling of periodically repeating solids by only considering the the smallest part of the crystal that can be translated periodically to produce the full pattern of the crystal, the unit cell (UC).

2.2 Kohn-Sham Equations

The Kohn-Sham (KS) equations offers a way to solve DFT. They are Schrödinger-like equations but approximate the effects of exchange and correlation in a way that only depend on the density. This simplifies the problem significantly if such a function is known because it uniquely defines an effective potential that compensates for the average interaction between particles. The particles are then treated as non-interacting fermions moving in this external potential. In turn this allows the Kohn-Sham wave functions to be expressed as a single Hartree-like function constructed from the solutions of the single particle energy eigenvalue problems for all the particles[6]. So the KS-equations are the one electron Schrödinger equations that generates the same density for a fictive system of non-interaction particles, as a system of real particles would. When expressed in this way the KS orbitals them selves have little physical meaning but the sum of orbital energies relates to the total energy of the system, see equation 2.8

The KS equation is in theory exact if we construct and deploy the "right" functional. Mathematically a functional is a mapping of a function onto a number. In density functional theory this functional is the exchange correlation functional (XC) and its purpose is to compensates for the average of these complicated interactions. The problem is that the exact form of the XC is not known for larger systems. However, it tuns out that we can get very accurate results even with crude first and second order approximations which only looks at the electron density or the gradient of the electron density at each point in space. This will be discussed more in the next section.

The KS wave function can be constructed by the lowest energy solutions to the eigenvalue equation (2.1), where v_{eff} is the fictitious external potential and ε_i is the orbital energy of the i'th KS-orbital ϕ_i.

$$\Big(-\frac{\hbar^2}{2m}\nabla^2 + v_{eff}(r)\phi_i(r)\Big) = \varepsilon_i\phi_i(r) \tag{2.1}$$

The denisty, ρ, in an N particle system is then:

$$\rho(r) = \sum_i^N |\phi_i(r)|^2 \tag{2.2}$$

The total energy functional E can then be written as:

$$E[\rho] = T_s[\rho] + \int dr v_{ext}(r)\rho(r) + E_H[\rho] + E_{XC}[\rho] \tag{2.3}$$

Where T_s is the kinetic KS energy, E_H is the Hartree energy, E_{XC} is the added energy from the XC-functional and v_{ext} is an external potential, which incorporates electron-nucleus interactions. The kinetic energy can be expressed in terms of KS-orbitals as:

$$T_s[\rho] = \sum_i^N \int dr\phi_i^*(r)\Big(-\frac{\hbar^2}{2m}\nabla^2\Big)\phi_i(r) \tag{2.4}$$

The Hartree energy is defined as:

$$E_H = \frac{e^2}{2}\int dr \int dr' \frac{\rho(r)\rho(r')}{|r-r'|} \tag{2.5}$$

The relation between the effective, also called the KS potential, and external potential can be expressed as:

$$v_{eff}(r) = v_{ext}(r) + e^2\int \frac{\rho(r')}{|r-r'|}dr' + \frac{\delta E_{XC}[\rho]}{\delta\rho(r)} \tag{2.6}$$

Where E_{XC} is the exchange correlation energy. The last term in equation (2.6) is known as the exchange-correlation potential,v_{XC}. It is formally the only unknown in KS DFT.

$$v_{XC}(r) \equiv \frac{\delta E_{XC}[\rho]}{\delta\rho(r)} \tag{2.7}$$

As stated earlier the KS orbitals are not real and do not correspond to the atomic orbitals in the system. However the sum of the orbital energies can be related to the total energy:

$$E = \sum_{i}^{N} \varepsilon_i - E_H[\rho] + E_{XC}[\rho] - \int \frac{\delta E_{XC}[\rho]}{\delta \rho(r)} \rho(r) dr \tag{2.8}$$

2.3 Different Functionals

Development of new and better XC functionals has been an essential part of the evolution of DFT as a computational method. Functionals are divided into different groups based on to what degree they approximate the functionals dependence on the electron density. Within each group there are deviations resulting from slightly different treatment of the approximate terms. One treatment of the approximation might capture the essential effects of one system better that another but the general accuracy within each family is comparable. However, between the different groups of functional there is a clear hierarchy where more advanced dependencies tend to better describe materials. This naturally comes with an increased cost in computational time. For a couple of decades numerical DFT was restricted to the the local density approximation (LDA). Where the energy functional only depends on electron density at each point in space. The XC-potential is then defined as the XC-potential a homogeneous electron gas with the same density would have at at that point. This is a very crude approximation but can yield surprisingly good results for systems with slow-varying densities like bulk solids. The next step on the hierarchical ladder of functionals is the generalized gradient approximation (GGA), which became available in the early 1990‘s. Here the functional do not merely depend on the magnitude of the electron density but also the gradient at each point. This group of functionals were able to account for more rapidly varying densities present in molecules. This quickly made DFT popular in the quantum chemistry community as well. Groups of functionals that use higher order derivatives of the electron density also exists, with meta-GGA being the next rung on the ladder. However, these generally have significantly higher computational cost, so both functionals used in this thesis are in the GGA-group.

For the first part of this study the Perdew-Burke-Ernzerhof (PBE) exchange-correlation functional was chosen. This is a functional known to give fairly good results with low computational cost. It is also a very commonly used functional, which allows comparison with other computational work. It preforms similarly to our other functional for single layer calculations, both regarding structure optimization and electronic properties. However, it fails to capture non-local correlation effects like vdW-forces as these are not incorporated within the standard framework of local (LDA) and and semi-local (GGA) XC functionals.

Because of this a fairly new functional was deployed. The vdW-DF-cx functional[7], developed to better model vdW-forces, essential in layered material systems like stacked COFs. This functional is in the greater family of vdW-DFs, which deviate from standard GGA functionals in the fact that the correlation depend on the density and the gradient of the density in a non-local manner. The vdW-forces are based on first principles and enables study of combined systems where both intra- and intermolacular forces are important. The family of functionals contain a more sophisticated approximation of the adiabatic connection formula (ACF), which includes the coupling-constant without an effective longitudinal dielectric function. The specific functional used in the second part of this study, the vdW-DF-cx, is one of the more recent additions the family of vdW-DFs. It is constructed as a general purpose functional, enabling the study of both vdW-bound and regular systems. It is know to yield good results for solids, layered materials and aromatic molecules[7].

The expression for the non-local correlation in vdW-DFT is given by:

$$E_c^{nl} = \int d^3r_1 \int d^3r_2 \rho(r_1)\phi(r_1,r_2)\rho(r_2) \tag{2.9}$$

Where ρ is the electron density. The exact form of ϕ depends on the separation r=|r$_1$-r$_2$| and two effective response parameters, which are functions of density and the gradient of the density in each point, respectively. At large separations we get a 1/r^6 dependence for ϕ while we recover a GGA-type correlation as we move closer.

2.4 Band Structure and Density of States

Band structure (BS) and density of states (DOS) are two fundamental ways to analyze and describe the electronic environment of materials. Isolated single molecules have certain discreet energy states which are allowed. A common example to demonstrate this is the calculation of the ground state energy of an electron in the hydrogen atom, within the Bohr model we can show this to be negative -13.6 eV, where the negative value confirms that the interaction between the proton and electron in the hydrogen atom is energetically favorable compared to having them as isolated particles. When we go towards larger systems with more atoms, energy states interact and blend together. They form energy bands that characterize the regions of energies allowed for electrons in the system. This easily allows characterization of materials into different groups like metals, semiconductors or insulators based one the character and placement of these energy bands. In the electronic band structure the total energy of the system is plotted against the different high symmetry reciprocal crystal directions while the density of states the energy is plotted against the the normalized number of states allowed at that energy. These allow us to understand where the electrons in materials lie energetically in the ground state and predict electronic transport properties of the system.

3

Methodology

3.1 Relaxation

The most fundamental part of any density functional theory calculation is to find or use the correct crystal structure for the system in question, as this is one of the only variables that can affect after selecting methods and XC-functional. Interesting physics can be studied while looking at hypothetical structures but if the aim is to capture and predict realistic effects, a energetically favorable structure is needed. Without a optimized crystal structure the computational results will not reflect the physics of the problem. For materials that are well known, crystal structure data and lattice constants may be available form crystallographic databases, but this was not the case when working with the fairly uncovered field of covalent organic frameworks. A reliable procedure for finding the correct crystal structure was therefore of utmost importance.

Finding the right crystal structure for any set of atoms theoretically is a hard task. DFT is a total energy method and the structure with the lowest total energy is the most stable if the chosen XC-functional captures all the physically important effects of the system in question. This means that one should ideally model every possible configurations of all competing phases in the relevant synthesis environment and compare the total energy while keeping in mind how the choice of functional may effect the relative energy of different configurations. This is an immense task for compounds with three and four different atoms, especially with carbon involved. Even before considering complicating entropy-driven effects from impurities or defects.

Luckily, with symmetry considerations and comparison with structural data on similar compounds we can get a good starting point. From there VASP has a wide variety of possible algorithms for structure optimization to aid in this process of creating the structure that minimizes the total energy. The type of procedure you want to use depends heavily on the state of the initial guess you put in. Since we work with highly symmetric organic compounds we have some constrains and guide lines for our initial guess. During the first trend study a reliable two-step relaxation process was developed. It allows for a fairly bad initial guess, based on structural data for the molecular components of the COFs in question like benzene or boroxide rings, to be feed in and tweaked to an optimized single layer crystal structure. In the first step a rough relaxation of the ionic positions are preformed with high tolerance for ionic movements (all forces were demanded to be under 30 meV/Å) and low accuracy for the total energy (change in energy was demanded to be bellow 10 meV between iteration steps) was used. This is combined with a conjugate-gradient algorithm to move the ions in the direction of steepest descent in the two-dimensional potential landscape, while fixing the ionic positions in the z-direction. This method possesses a very reliable backup routine, which is important to avoid divergence that crashes the numerical calculation. In the second step we assume that a better guess for the crystal structure is found. A finer relaxation were then preformed with lower tolerance for ionic movements (all forces were demanded to be under 10 meV/Å) and higher accuracy for the electronic ground state (change in energy was demanded to be bellow 0.1 meV between iteration steps). Deploying the quasi-Newton algorithm[8] to relax the ions to the proper ground state position. This process is known to be fast and accurate if the initial guess of the ionic positions is close to the local minimum, hence the reason why we preformed the initial rough relaxation.

When we relaxed the structures we allowed VASP to alter ionic positions and change the UC shape but not the total volume of the UC. Therefore, any alteration of the UC size or shape in the in-plane directions will come at the cost of adding or subtracting vacuum between the periodically separated slabs. However, if vacuum layer length is well converged the change in total energy with addition or subtraction of small amounts of vacuum is so small that the structures have room for improvement.

A small external pressure was present after the final relaxation procedure. This is believed to be artificially produced by the periodic boundary conditions used in the calculations. A series of tests were preformed on this matter but it is not believed to cause any noticeable changes to the parameters we are interested in.

3.2 Convergence Testing

The second step of any DFT analysis is convergence testing of relevant input parameters. Convergence testing was performed with respect to energy cut-off, vacuum level, k-point density, and maximal force, within specific convergence criteria.

The energy cutoff was the first parameter that was tested for convergence. The change in relative total energy of one UC the structure pairs was demanded to be within 3 meV, with a step size of 50 eV. COF-1 was compared to CTF-1, while COF-1X was compared to CTF-1X. Comparing the relative change in total ground state energy assures us that our results are consistent throughout the sample materials. As the same types of atoms and bonding types are also present in the larger COFs these results are expected to be consistent also for the larger COFs. The maximal forces and pressures were simultaneously checked to be within 0.05 eV/Å and 3 Kbar respectively, with the same energy cutoff step size. These parameters converged much more rapidly, so the relative energy was the limiting factor. The relative energy convergence test showed that a sufficient cutoff was found to be 450 eV. However, in the final calculations which are presented in the thesis an energy cutoff of 500 eV was chosen, as this was the default recommended value for compounds containing carbon and the increase in computational time was small. For volume relaxation Energy cutoff was increased by 30%. This is recommended as a larger basis set is needed to accommodate the dynamic size change of the UC.

After a sufficient cutoff energy was established, k-point density was tested for convergence. The change in total energy was demanded to be less than 1 meV when increasing the k-density by one in the two directions of the plane. The k-point meshes that were tested was (1,1,1), (2,2,1), (3,3,1), (4,4,1). The result of the convergence test was that a k-point mesh of (2,2,1) was sufficient for the two pairs of structures, COF-1 vs. CTF-1 and COF-1X vs. CTF-1X, to get the change in energy bellow the desired convergence criteria. However, for the final calculation the k-point mesh was increased to (3,3,1) for relaxation and self-consistent calculations, as this only adds a slight increase in computational time and can only increase accuracy. For the stacked structures the k-point density was increased to (3,3,3), as a shorter wave vector in the z-direction has to be resolved more finely in reciprocal space. The single layer k-point density was increased to (3,3,2) for the self-consistent density of states calculations, as the tetrahedron method with Blöchl corrections k-point scheme was deployed, which requires at least two k-points in each direction. For the final non-self-consistent calculations, that produce BS and DOS plots, a much larger k-point density was used to get a better resolution. The non-self consistent calculations use the charge density from the self-consistent calculations. This allow for a large k-point density while keeping the computational time low. For the band structure 15 k-points were used along each line between high-symmetry points. For the single layer DOS a gamma-centered k-point mesh of (6,6,2) was used. Also here the k-point density in the z-direction was increased significantly to (6,6,24) when moving over to the stacked structures. This is because we want to accommodate for the shorter wave vector corresponding to the z-direction.

Since VASP uses periodic boundary conditions we need to preform convergence testing of the energy with respect to the length of the vacuum layers. We want to find the smallest distance the periodically spaced sheets can have without interacting with neighboring layers. This is because we want to model isolated single layers but keep the UC volume as small as possible to reduce computational time. Like we did with the energy cutoff this was done by comparing the relative change in energy of the two pairs of structures when increasing the vacuum layer by a step size of 2 Å. The change in relative energy was then demanded to be below 1 meV. The result of the convergence test was that a vacuum level of 10.5 Å was sufficient. The results of the convergence testing showed promising results for further study, since we saw that both pairs of structures converged within our criteria for the same energy cut-off and vacuum level length. This enables us to compare the different structures on equal footing while maintaining low computational cost.

3.3 Band Structure and Density of States

The band structures and density of states plots were calculated in a two-step process after the structures were relaxed. The first step was a self-consistent calculation to get the correct charge density, then a non-self-consistent calculation that uses the calculated charge density from the previous run, new k-points are introduced for increased accuracy. The tetrahedral method with Blöchl correction was used to determine the partial occupancies of the orbitals for the DOS calculations. The band structures were calculated with 15 k-points for each line between the high symmetry points. The chosen stacked-structure band paths are appropriate to represent the full electronic band structure of AA-stacked COF-1, which has the P-62m space group (number 189). It does not show full path for the AA*-stacked structures, as the process of tilting of the out of plane UC vector reduces the symmetry operations available in the UC, making new paths unique. We have still chosen to plot the BS with the same path for comparison. We can allow this because these paths at least contain the two most important parts of the band structure, the valance band minimum (VBM) and conduction band maximum (CBM). For the single layer BS we only show the part of the path that in reciprocal space correspond to the in plane directions. Compared to the layered structures where we show the same path at the beginning, then move in the reciprocal out-off-plane direction when going from high-symmetry points Γ to A, before walking a triangular path, similar to the single layer path there.

For some of the single layer DOS plots the amount of grid points should have been significantly increased as the most narrow bands are not resolved in some of the structures. This is the case for COF-1X, CTF-1Y, COF-15 and TP-COF, seen in Figures A.1,A.3,A.6 and A.9 in the Appendix. The bands are visible in the BS plots.

3.4 Stacking

In the stacking study different stacking configurations of the COFs have been explored. One can imagine a solid stack of COFs like a deck of cards, were 2D-sheets are separated by a fixed perpendicular distance, the inter layer distance. We wanted to find out how adjacent layers lie compared to each other in order to achieve the lowest total energy.

The configuration were adjacent layers are placed directly on top of each other, so that atoms in one layer lies closest to their equal counterparts in the next, is called the AA-stacking configuration. Earlier experimental works on COFs have predicted this to be the optimal structure for some of our candidate materials. This was later refused in [9] where they present stacking studies with results similar to ours. We wanted to test this so for every COF separate series of calculations have been preformed were we start of with the AA-stacking configuration and then in subsequent calculations move every layer a small amount in symmetry unique directions. In practice this is done by tilting and extending the out of plane UC-vector of the hexagonal AA UC. In the deck of cars analogy this will correspond to tilting the deck of cards, like you would do in the game of solitaire to make the edge of every card visible. The difference is of course that within our calculations we deploy periodic boundary conditions so the sheets are considered infinitely large and edges are not considered. What we get then is a stack of COFs were every layer is translated a fixed amount in a fixed direction compared to the one above or bellow. To define these structures we assign them with the translation vector in plane like AA*(x,y). Where AA* signalizes that the structure is displaced away from the AA configuration and the (x,y) coordinates define the distance that every layer is displaced in the plane in Å. We have chosen to define the axis so that the x-coordinate is perpendicular to one of the linker directions while the y-axis is parallel. 209 different symmetry unique AA* configurations have been calculated for each COF in order to map the complete landscape of AA* translations. The mappings were done with a constant interlayer distance of 3.35 Å, which was the optimal interlayer distance of optimally AA*-stacked COF-1.

We have made a few assumptions and simplifications in order to achieve the results of this stacking study. First we have only translated the layers and not assessed rotation at all. This is because all stable configurations have a large area of overlap with adjacent layers as the vdW-interaction between layers is then energetically favorably.

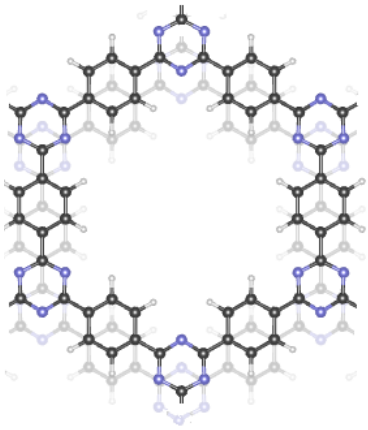

Figure 3.1: Illustrated here is one pore of optimally AA-stacked CTF-1. Every layer is translated a fixed distance 1.82 Å compared to the next along one of the directions parallel to the linker as suggested by the stacking study results.*

3.5 Precursor Calculations

In the precursor calculations the total energy of stacked and single layer COF-1 was compared to that of their chemical precursor molecule, BDBA. The net reaction for creating one UC of COFs can be seen in Equation 1.1. The isolated single molecules were relaxed much in the same way as the single layer COFs, except they had a layer of vacuum in all directions. The same criteria for energy and force convergence were used, as well as the same functional, in order to compare the results on equal footing. The ground state energies of three molecules of BDBA were compared with the added energy of six water molecules and either optimally AA*-stacked or single layer COF-1.

4

Results

4.1 Total Energy and Stability

Simple total energy calculations comparing COF-1 to its chemical precursor molecules were performed after the *AA**-stacking study was concluded. The complete setup is mentioned in the methods part. This reveled that COF-1 is stable when stacked but not as freestanding single layers. The total energy of the stacked COF-1 was 0.35%lower than the energy of the precursors while the energy of the single layers were 0.25%higher. This corresponds to an energy differences of 21 meV/atom and 15 meV/atom, respectively. These are small but significant energy differences. It is hard to know the validity of these calculations, they should ideally have been performed using a costlier hybrid functional, which are generally known to do better in these types of energy comparisons. We also note that some additional stability could arise from further optimization of the crystal and that all the systems can be stabilized further in specific synthesis environments. The pores can be stabilized by guest molecules, the precursor molecules can be stabilized by intermolecular forces in solution and the single layers, which we modeled as isolated sheets, can be supported by a fitting substrate. It is hard to asses these energy corrections directly or if they would be strong enough to tip the scales of the relative energies from the precursor calculations. However, if it turns out that the relative stability of these systems is correct, then this has significant implications. First, this means that COF-1 is unstable as freestanding single layers, which is often the case for 2D-materials like this but not in the case of the well-known "mini-frameworks" graphene or boron nitride. This means that interesting physics, which often arises in proper 2D-materials like this, unfortunately cannot be studied. Second, this instability can seriously affect the growth of these frameworks, as they might not be thermodynamics stable before they form several layers. This might prevent the formation reaction completely or slow it down drastically. This is relevant information if you are trying to synthesize these frameworks. It might restrict the number of possible synthesis routs and possible suitable substrates. Third, it may facilitate in the formation of high quality crystals as the reaction involved will have good reversibility because of the small energy barriers. The energy difference is however so low that a strong vdW-stabilizing substrate might allow single layer synthesis, as is claimed in [10], where a single layer coverage of COF-1 on graphite is reported to trap fullerene (C_{60}) molecules.

Table 4.1: Unit cell parameters and range of bond lengths for single layer COFs. Calculated with the vdW-DF-cx functional.

COF	Cell Vector Length [Å]	Cell Area [Å^2]	C-C Bond Lengths [Å]	C-B/N Bond Lengths [Å]	C-H Bond Lengths [Å]	B-O Bond Lengths [Å]
COF-1	15.15	198.83	1.39-1.41	1.56	1.10	1.39
COF-1X	22.70	447.05	1.39-1.49	1.55	1.09-1.10	1.39
COF-1Y	30.28	794.10	1.39-1.48	1.55	1.09-1.10	1.39
CTF-1	14.56	183.53	1.39-1.48	1.35	1.09	None
CTF-1X	22.11	423.51	1.39-1.48	1.35	1.09	None
CTF-1Y	29.68	762.67	1.39-1.48	1.35	1.09	None
COF-5	30.21	790.33	1.37-1.46	1.54	1.09	1.40
COF-10	37.77	1235.73	1.37-1.49	1.54	1.09-1.10	1.41
COF-15	45.34	1780.32	1.37-1.48	1.54	1.09-1.10	1.41
PPy-COF	22.53	439.42	1.37-1.44	1.56	1.10	1.39
PPy-CTF	21.92	416.49	1.37-1.48	1.35	1.09-1.10	None
TP-COF	38.22	1222.35	1.37-1.46	1.54	1.09-1.10	1.40

4.2 Crystal Structure

Our previously described relaxation procedure was performed for all twelve structures and converged within specified convergence criteria. It yielded good results with symmetry equivalent bond lengths varying less than 1e-5 Å for all materials. We believe that this is sufficient to not cause noticeable changes in the interesting parameters. However, if the error is one or two orders of magnitude larger we expect that this can cause problems. The calculated bond lengths can reliably be compared internally but is not directly relatable to experimental bond lengths or other theoretical work as they dependent on the level of theory and type of functional used in the calculations.

4.3 Band Structure and Density of States

Both the PBE and vdW-DF-cx functional consistently underestimate the magnitude of the electronic band gap. Other functionals include an empirically based fraction of exact Fock-exchange on top of the GGA XC-functional to cope with this problem but these are still quite costly to deploy in wider studies. As a crude rule of thumb we can expect the band gap with our functionals to be up to twice as large as our results in the band gap table (Table 4.2), BS and DOS plots, show. Or at least closer to this then what is presented. This can depend heavily on the system in question but we are hopefully safe when comparing materials with resembling structures and similar type of bonding. However, one should be care full assuming that the same scaling of this error is present when comparing single layer and stacked structures. Nevertheless, we can expect that other properties of the BS and DOS can give use information about this class of materials as a whole. The variations in band gap between the different structures and the type of band gap (direct/indirect) can be compared. As well as the band widths and curvatures.

In Figures **??**-**??** and **??**-**??** BS and DOS for single layer and optimally AA*-stacked COF-1, CTF-1 and COF-1Y are shown together for comparison. The BS and DOS plots for the rest of the structures can be view in the appendix. We see that all single layer structures have fairly large band gaps, well into insulator range when considering the underestimation from the functional. When moving from Figures **??** to **??**, extra phenyl rings are added to the linker. This consistently reduces band gaps and widths for both the COF-1 and the CTF-1 sets of structures. The band structures have been plotted with the same axis in order to visualize the difference in curvatures. We see many similarities between the figures. A thing to notice is the existence of flat or very narrow bands. Our calculations showed flat conduction bands for all single layer structures, except for CTF-1, which has some dispersion both in the valance band and conduction band.

The DOS plots for the single layer structures contain tall and narrow spikes. This is a sign of localized state. This is a common sight in covalently bonded molecular-like crystals. They resemble a middle ground between the discreet states of isolated molecules and the typical wide bands of regular condensed matter

Our calculations showed some slight dispersion for single layer CTF-1, but for COF-1 and the other larger structures the bands are very narrow. This is in agreement with other theoretical work [3] on similar structures composed of only carbon and hydrogen, where they concluded that the inclusion of more phenyl groups on the liker resulted in narrowing of the bands. In [11] the band structure of COF-1 and CTF-1 was calculated with DFT. They showed band structures with all the same features as our calculations, but there were small differences in band gap. However they do not report which XC-functional they used for these specific calculations which makes them comparison impossible.

In the band structures of the materials we see a lot of similarities. This is to be expected as they have similar crystal structures and bonding with the same type of covalent nature. In all structures we see that somewhere around the fermi level there are flat bands, this adds to the insulating behavior of the materials as flat bands have a very high effective mass/low mobility. Flat bands have also been reported in a class of COFs with the kagome lattice motif [3]. In the structures that have a flat valance band we can neglect hole conductance and equally for the structures with flat conduction bands we can neglect electron conduction. This can be utilized in single pole electronic devices where one type of carrier is preferred.

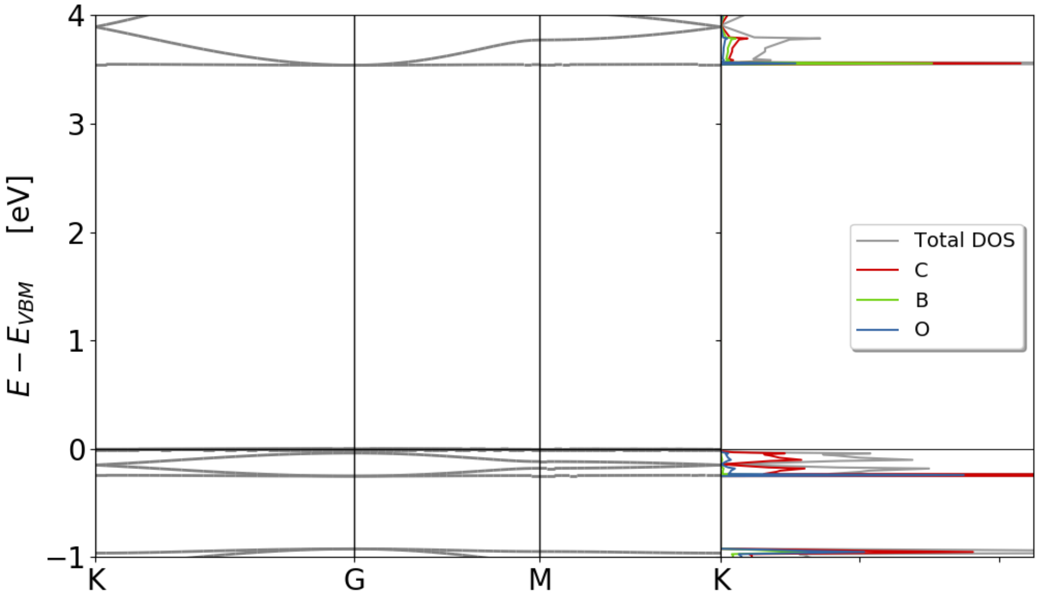

Figure 4.1: Band structure and elemental density of states for single layer COF-1. Single layer COF-1 has the largest band gap of all the candidate materials. Calculated using the vdW-DF-cx functional.

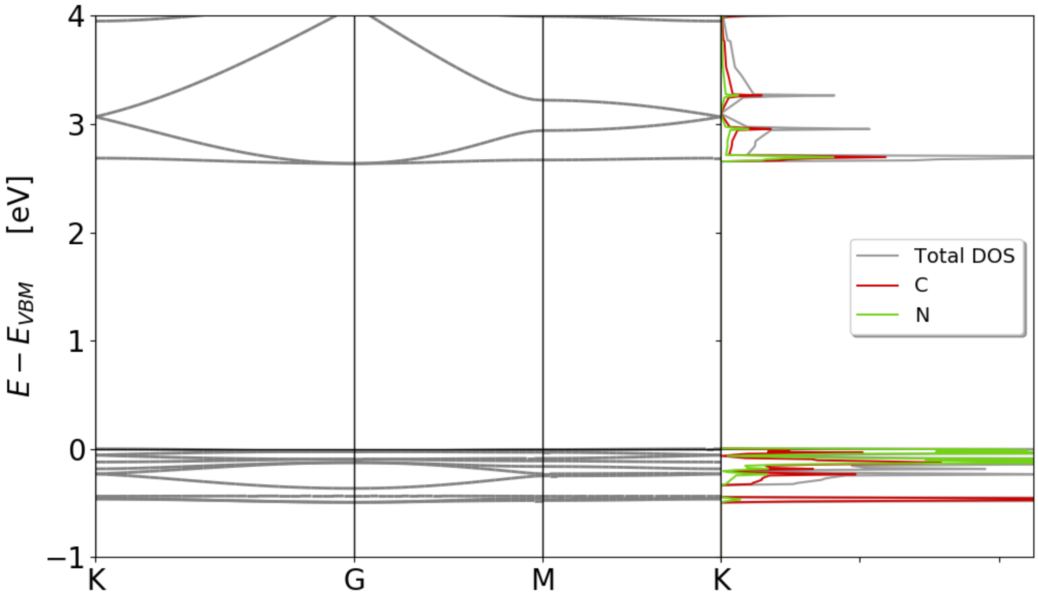

Figure 4.2: Band structure and elemental density of states for single layer CTF-1. The Band gap is lower and the band widths are higher in CTF-1 compared to COF-1. Calculated using the vdW-DF-cx functional.

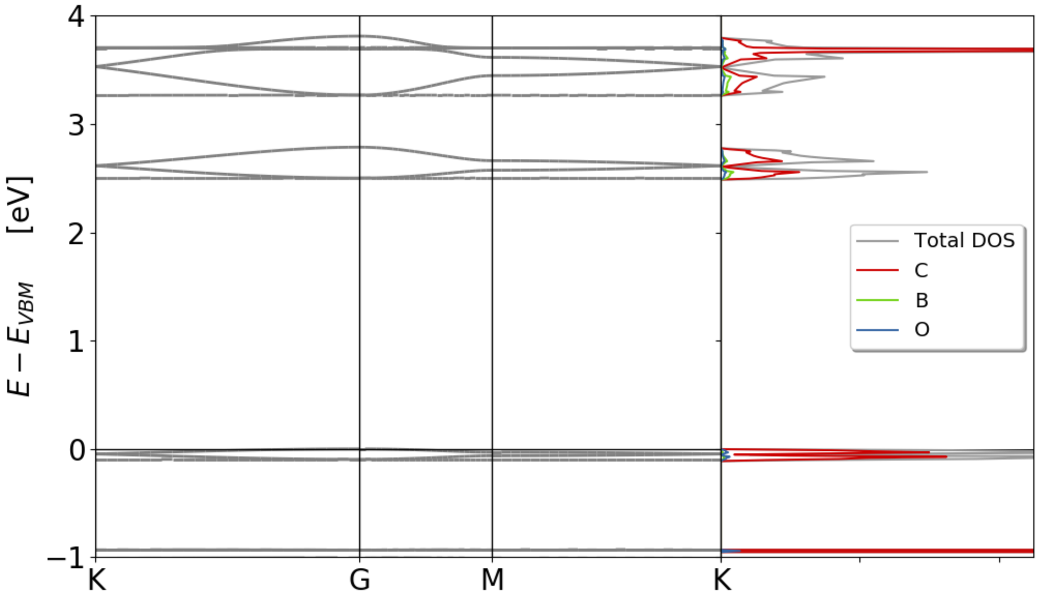

Figure 4.3: Band structure and elemental density of states for single layer COF-1Y. COF-1Y has similar features to that of COF-1, expect that all the bands are squeezed together. Calculated using the vdW-DF-cx functional.

Table 4.2: Comparison of the band gaps of single layer and stacked structures

COF	Single Layer Band Gap [eV]	Optimally AA*-Stacked Band Gap [eV]
COF-1	3.56	2.73
COF-1X	2.83	2.25
COF-1Y	2.50	1.71
CTF-1	2.66	2.14
CTF-1X	2.44	1.89
CTF-1Y	2.22	1.70
COF-5	2.49	1.89
COF-10	2.33	1.77
COF-15	2.25	1.72
PPy-COF	2.44	1.77
PPy-CTF	2.00	1.41
TP-COF	2.56	1.89

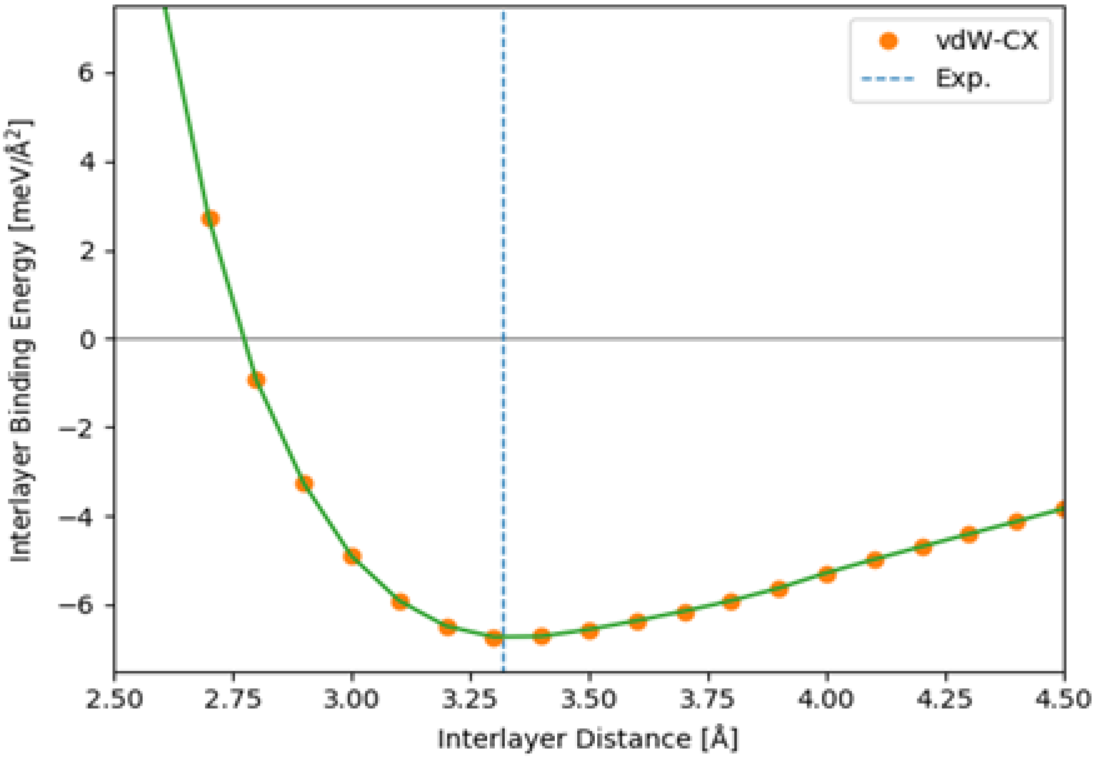

Figure 4.4: The tug of war between the stabilizing vdW-interactions and repulsive forces cause by overlap of orbitals are clearly shown when the total energy of the optimally AA-stakced COFs are calculated with different interlayer distances. The forces stabilize at a equilibrium distance of 3.34 Å, close to the experimentally reported value of 3.32 Å. [12]*

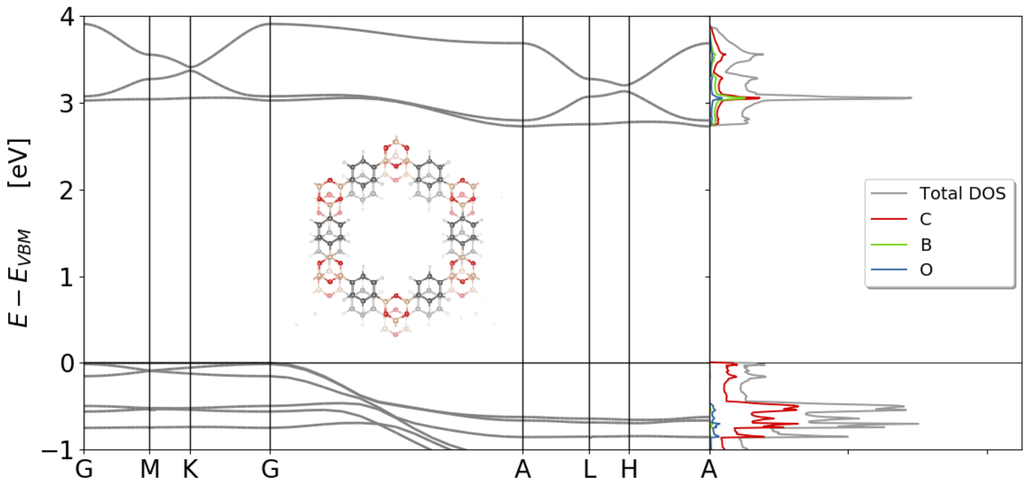

Figure 4.5: Band structure and elemental density of states for optimally AA-stacked COF-1. The insert in the band gap illustrate how two layers would stack. We see the dispersion in the bands when going from Gamma to A, which corresponds to the out of plane direction in real space. Calculated using the vdW-DF-cx funtional.*

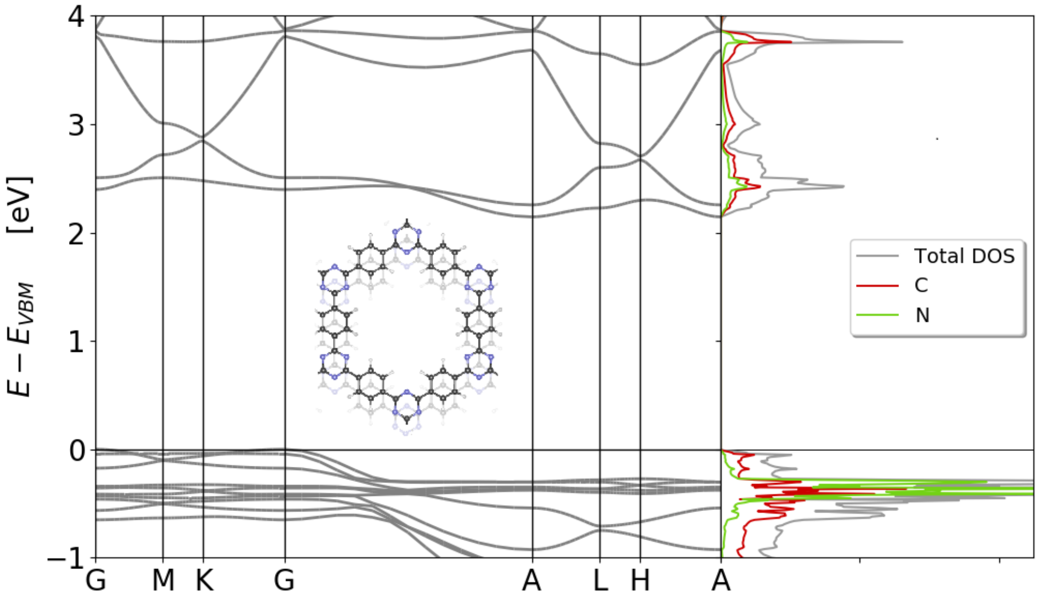

Figure 4.6: Band structure and elemental density of states for optimally AA-stacked CTF-1. The insert in the band gap illustrate how two layers would stack. Features are still similar to that of COF-1 but the bands are much broader. Calculated using the vdW-DF-cx funtional.*

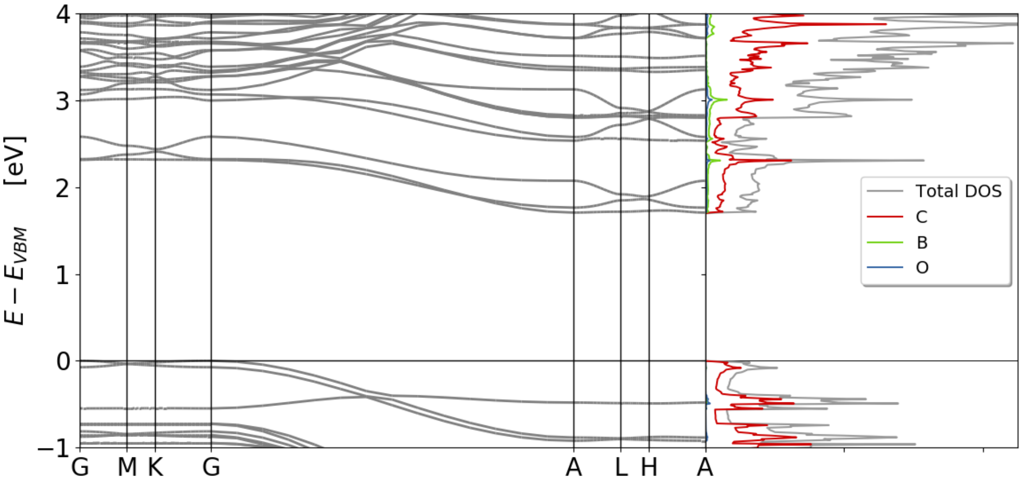

Figure 4.7: Band structure and elemental density of states for optimally AA-stacked COF-1Y. The same trends applies when going from COF-1 to COF-1Y for the stacked structures, Bands get pinched when adding extra phenyl-rings to the linkers. Calculated using the vdW-DF-cx funtional.*

4.4 Stacking Study

The results of the stacking study can be seen in Figure 4.8 to 4.10. The figures represent the possible landscape of AA*-stacking varieties for the selective COFs. Because of the hexagonal symmetry of the COFs in question we see that these images have six-fold rotational symmetry around the center. The origin in these figures represents the simplest possible stacking, a perfect AA-stacking, where subsequent layers are placed directly on top of each other so that equal atoms in neighbouring layers have the smallest possible distance between them. We can see that the stable low energy region from white to red lie in circle close to the origin. However, in most figures this is actually the global energy maximum, so the worst possible AA*-structure. This is most easily seen in Figure 4.8 (a) where the circles in the inner region show a steep rise in energy. These figures show that the stacking arrangement is a trade-off between stabilizing vdW-forces and Pauli repulsion. In the AA-configuration the vdW-forces are maximized since equal atoms in neighbouring layers are only separated by the interlayer distance which is fixed but the Pauli repulsion from overlapping π-orbitals of the double bonds overshadow this effect and dominates, making the configuration unfavorable. On the other end of the spectrum we have the regions around the stable centre. Here the average distance to the the closest atoms in the neighboring layer is lower so that the stabilizing vdw-effect is much weaker.

The optimal AA*(x,y)-stacking arrangements and the optimal interlayer distance in those arrangements are presented in Table 4.3. The xy-coordinates come from the energy minimums in the Stacking study (Figures 4.8-4.10) and the interlayer distances are achieved the same way as presented in Figure 4.4.

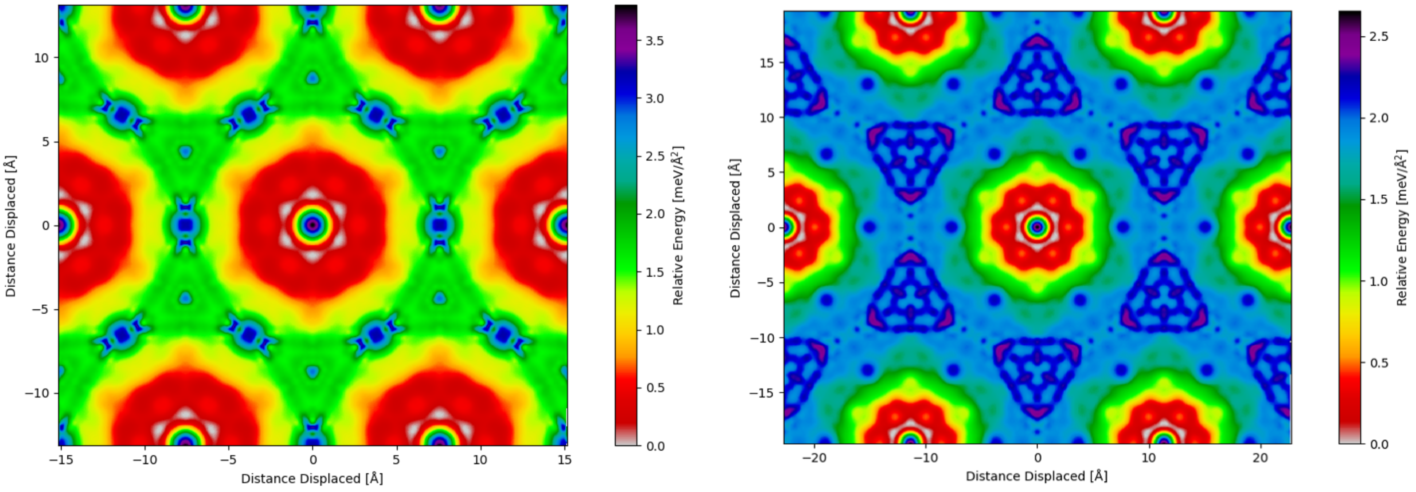

(a) COF-1 (b) COF-1X

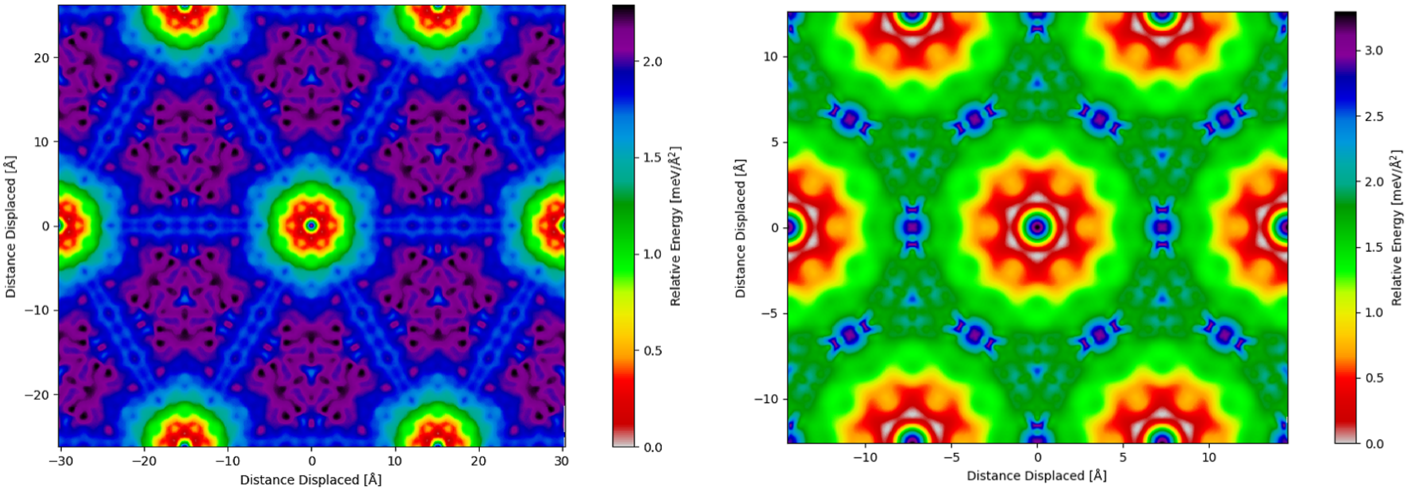

(c) COF-1Y (d) CTF-1

Figure 4.8: Cubic interpolation of the AA-stacking landscape for each COF. The exotic color-scheme is chosen because it finely resolves the upper and lower part of the energy range.*

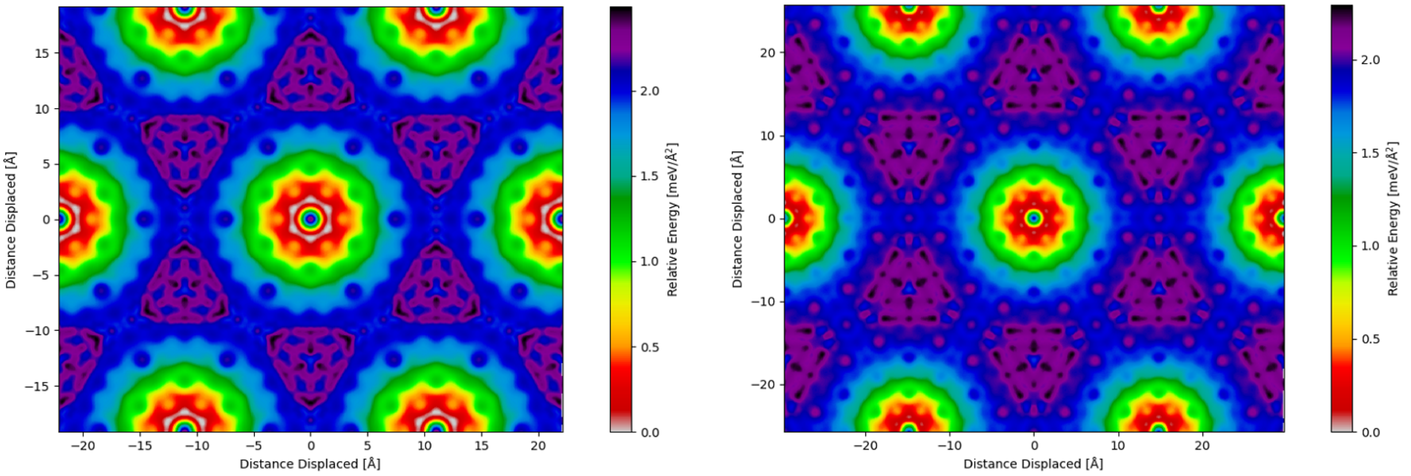

(a) CTF-1X

(b) CTF-1Y

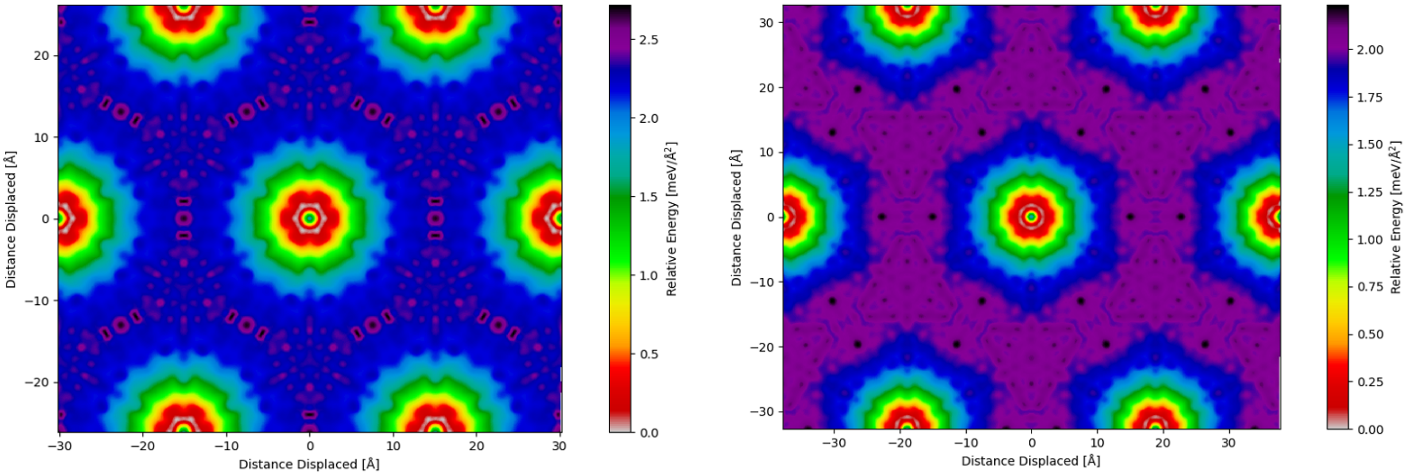

(c) COF-5

(d) COF-10

Figure 4.9: Cubic interpolation of the AA-stacking landscape for each COF*

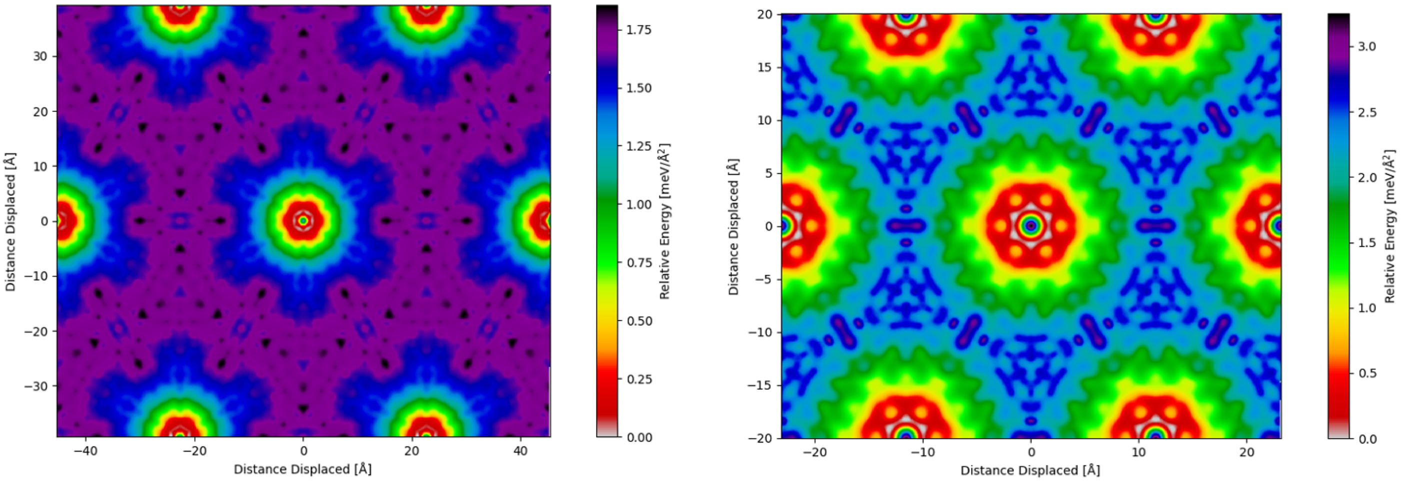

(a) COF-15 (b) PPy-COF

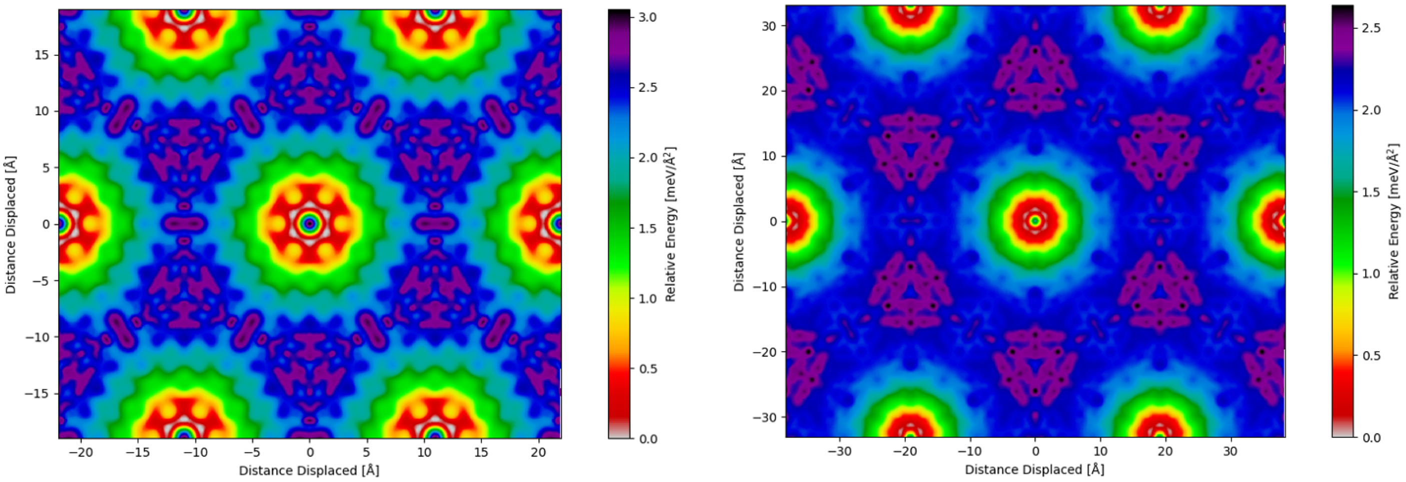

(c) PPy-CTF (d) TP-COF

Figure 4.10: Cubic interpolation of the AA-stacking landscape for each COF*

Table 4.3: Optimal AA(x,y)-stacking arrangements and interlayer distance. Calculated with the vdW-DF-cx functional.*

COF	Optimal AA*(x,y)-Stacking Configuration [Å]	Optimal Interlayer Distances AA*-Stacked Configuration [Å]
COF-1	(0,1.875)	3.34
COF-1X	(0,1.920)	3.35
COF-1Y	(0,1.650)	3.41
CTF-1	(0,1.712)	3.35
CTF-1X	(0,1.750)	3.43
CTF-1Y	(0,1.712)	3.36
COF-5	(1.732,0)	3.35
COF-10	(0,1.742)	3.36
COF-15	(1.678,0)	3.37
PPy-COF	(0,1.850)	3.35
PPy-CTF	(0,1.668)	3.37
TP-COF	(0,1.750)	3.36

5

Conclusions

5.1 Electronic Properties

The results for the single layers structures show that both band gap and band width consistently goes down as more phenyl-rings are added to the linkers. The reduction of the band gap per added phenyl-ring, both in terms of relative change in magnitude and percentage decrease, were biggest amongst the COFs with the boroxide node (COF-1, COF-1X and COF-1Y) and smallest for the COFs with the TP-node (COF-5,COF-10,COF-15). The relative difference in band gaps between the structures with three-membered phenyl-chains are also much smaller than for the structures with the single phenyl-ring linker. When combining the PPy-linker with the three nodes a small reduction is seen for the structures with boroxide node, while a significant decrease and increase is seen for the triazine- and TP-nodes, respectively.

The same trends apply when adding more phenyl-rings to the linkers of stacked structures. Bands retain the same overall features but the width is narrowed and band gap energies decrease. Also for the stacked structures the biggest decrease in band gap, relative and percentage-wise, were seen in the group with the boroxide node but this time it was enough to make the band gap of the three three-phenyl-ring structures approximately equal (1.70-1.72 eV). Strong dispersion is seen in the reciprocal k-direction that corresponds to the out of plane direction in real space when plotting the band structures of the stacked materials. This can be attributed to the alignment of π-conjugated molecular components, facilitating transport in the out of plane direction. This is interesting in of itself, as single crystals can display direction dependant conductivity.

5.2 Stacking

The results from the stacking study showed that the most optimal AA*-stacking was when every layer is shifted a small distance away from perfect hexagonal AA-stacking, as we can see from the white and red regions in the center of the interpolation figures (4.8-4.9). The specific shape of the electron cloud determines the optimal configuration but it is a trade-off between stabilizing vdW-interactions and Pauli repulsion. This creates symmetrical interlocking patterns which are determined by the shape of the linkers and nodes, as we saw an example of in Figure 3.1..

5.3 Stability

The COFs might not be stable as free standing single layers but the stabilizing effects from interlayer interaction or a strong interaction to a substrate might can enough to lock them in place. The layered frameworks might also be stabilized by incorporation of guest species or addition of different functional groups inside the pores. This offers the possibility to tailor these frameworks on different levels, Increasing the overall tuneability, which is an important aspect when designing specialized components for electronic or opto-electronic devices. For example by combining the frameworks with different substrates or in specific hetrostructures or by introducing guest species and dopants in the form of molecules, metal-ions or even small diameter nanotubes.

Bibliography

[1] Adrien P. Côté, Annabelle I. Benin, Nathan W. Ockwig, Michael O&#039;Keeffe, Adam J. Matzger, and Omar M. Yaghi. Porous, crystalline, covalent organic frameworks. *Science*, 310(5751):1166, Nov 2005. doi:10.1126/science.1120411. URL `http://science.sciencemag.org/content/310/5751/1166.abstract`.

[2] Hiroyasu Furukawa, Kyle E. Cordova, Michael O'Keeffe, and Omar M. Yaghi. The chemistry and applications of metal-organic frameworks. *Science*, 341(6149), 2013. ISSN 0036-8075. doi:10.1126/science.1230444. URL `https://science.sciencemag.org/content/341/6149/1230444`.

[3] Jean-Joseph Adjizian, Patrick Briddon, Bernard Humbert, Jean-Luc Duvail, Philipp Wagner, Coline Adda, and Christopher Ewels. Dirac cones in two-dimensional conjugated polymer networks. *Nature Communications*, 5:5842 EP –, Dec 2014. URL `http://dx.doi.org/10.1038/ncomms6842`. Article.

[4] Jia Guo, Yanhong Xu, Shangbin Jin, Long Chen, Toshihiko Kaji, Yoshihito Honsho, Matthew A. Addicoat, Jangbae Kim, Akinori Saeki, Hyotcherl Ihee, Shu Seki, Stephan Irle, Masahiro Hiramoto, Jia Gao, and Donglin Jiang. Conjugated organic framework with three-dimensionally ordered stable structure and delocalized p clouds. *Nature Communications*, 4:2736 EP –, Nov 2013. URL `http://dx.doi.org/10.1038/ncomms3736`. Article.

[5] Haining Liu, Qing Li, Yiming Zhu, Mei Zhang, Runjing Liu, Xiaoming Li, Xiao Kang, Zheng Li, and Shanlin Qiao. Synthesis and mechanical exfoliation of imine-linked two-dimensional conjugated polymers. *J. Mater. Chem. C*, 6:722–725, 2018. doi:10.1039/C7TC04370H. URL `http://dx.doi.org/10.1039/C7TC04370H`.

[6] W. Kohn and L. J. Sham. Self-consistent equations including exchange and correlation effects. *Phys. Rev.*, 140:A1133–A1138, Nov 1965. doi:10.1103/PhysRev.140.A1133. URL `https://link.aps.org/doi/10.1103/PhysRev.140.A1133`.

[7] Kristian Berland, Calvin A. Arter, Valentino R. Cooper, Kyuho Lee, Bengt I. Lundqvist, Elsebeth Schröder, T. Thonhauser, and Per Hyldgaard. van der Waals density functionals built upon the electron-gas tradition: Facing the challenge of competing interactions. , 140:18A539, May 2014. doi:10.1063/1.4871731.

[8] Convergence acceleration of iterative sequences. the case of scf iteration. *Chemical Physics Letters*, 73(2):393 – 398, 1980. ISSN 0009-2614. doi:https://doi.org/10.1016/0009-2614(80)80396-4. URL `http://www.sciencedirect.com/science/article/pii/0009261480803964`.

[9] Lukose Binit, Kuc Agnieszka, and Heine Thomas. The structure of layered covalent-organic frameworks. *Chemistry – A European Journal*, 17(8):2388–2392, 2011. doi:10.1002/chem.201001290.

[10] Daling Cui, Jennifer Macleod, Maryam Ebrahimi, Dmitrii Perepichka, and Federico Rosei. Solution and air stable host/guest architectures from a single layer covalent organic framework. *Chemical communications (Cambridge, England)*, 51, 09 2015. doi:10.1039/c5cc07059g.

[11] Rico Gutzler. Band-structure engineering in conjugated 2d polymers. *Physical chemistry chemical physics : PCCP*, 18, 10 2016. doi:10.1039/c6cp06101j.

[12] Binit Lukose, Agnieszka Kuc, Johannes Frenzel, and Thomas Heine. On the reticular construction concept of covalent organic frameworks. *Beilstein Journal of Nanotechnology*, 1:60–70, 2010. ISSN 2190-4286. doi:10.3762/bjnano.1.8.

Appendices

A

Appendix 1

A.1 Single Layer BS and DOS

This appendix includes all BS and DOS figures, which are not included in the main text.

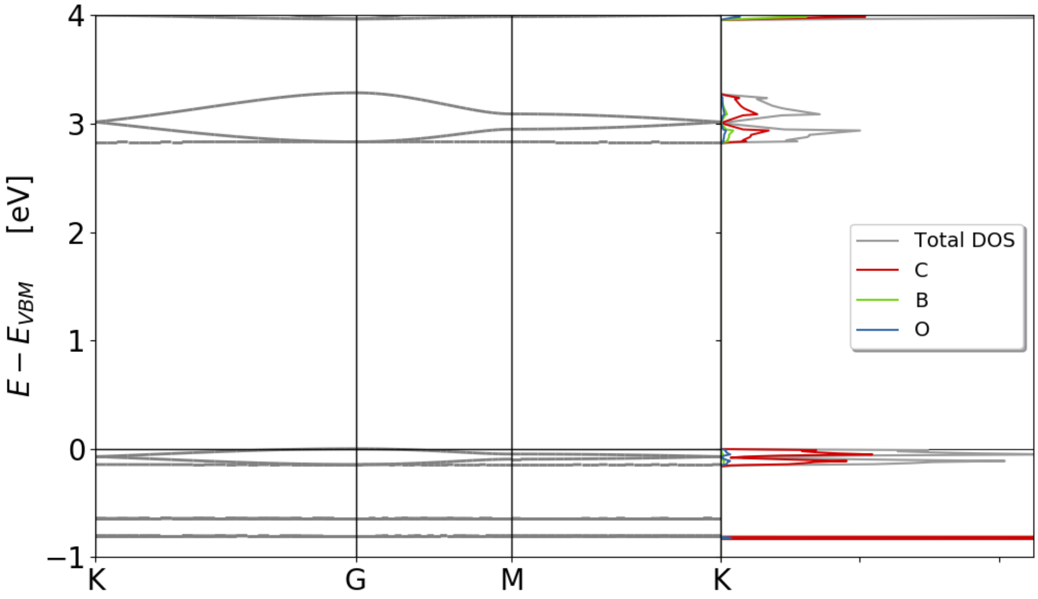

Figure A.1: Band structure and elemental density of states for single layer COF-1X. Calculated using the vdW-DF-cx functional.

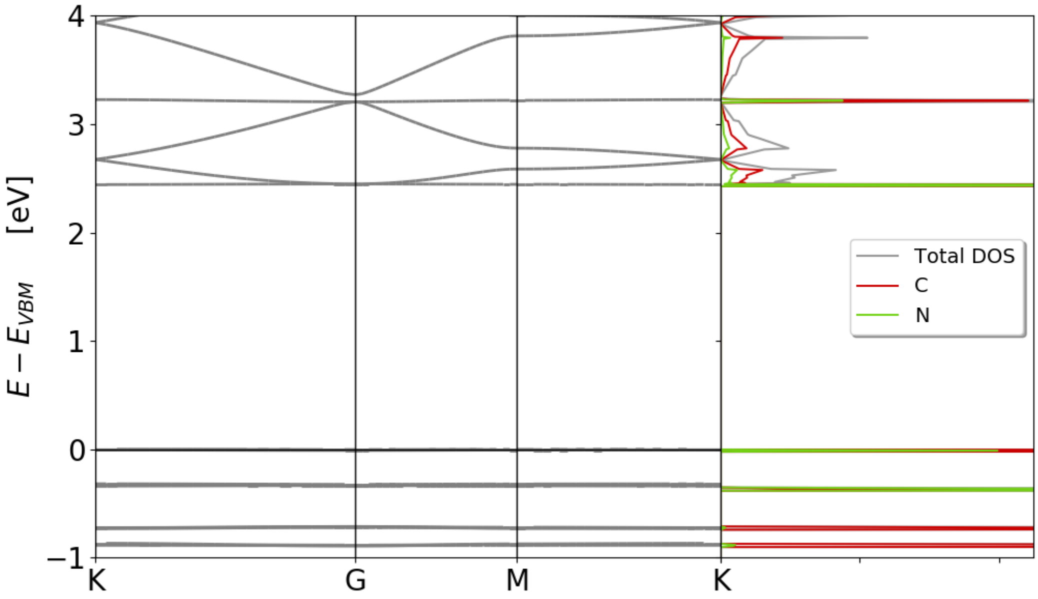

Figure A.2: Band structure and elemental density of states for single layer CTF-1X. Calculated using the vdW-DF-cx functional.

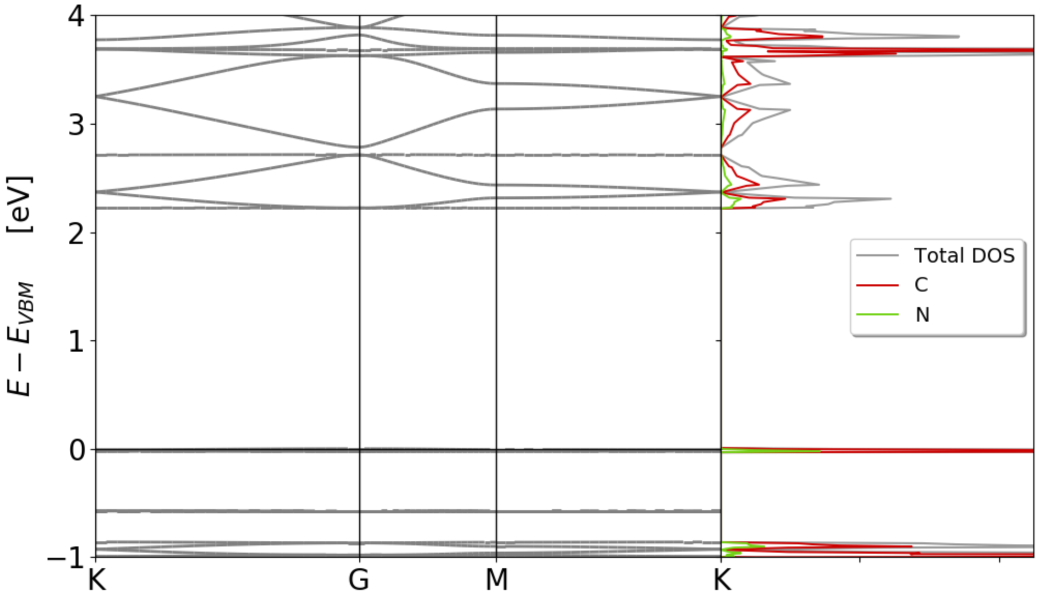

Figure A.3: Band structure and elemental density of states for single layer CTF-1Y. Calculated using the vdW-DF-cx functional.

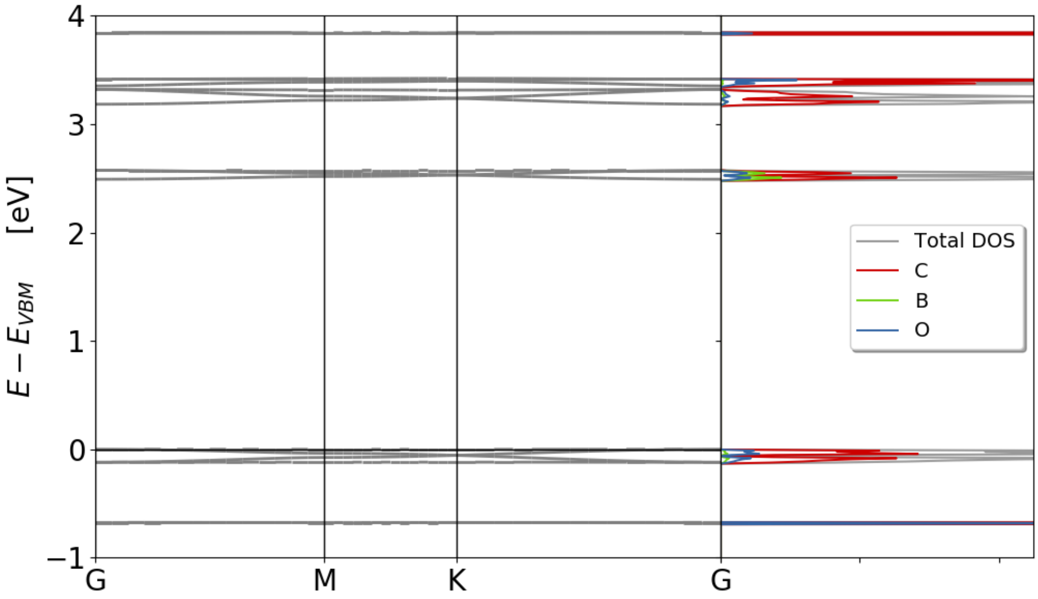

Figure A.4: Band structure and elemental density of states for single layer COF-5. Calculated using the vdW-DF-cx functional.

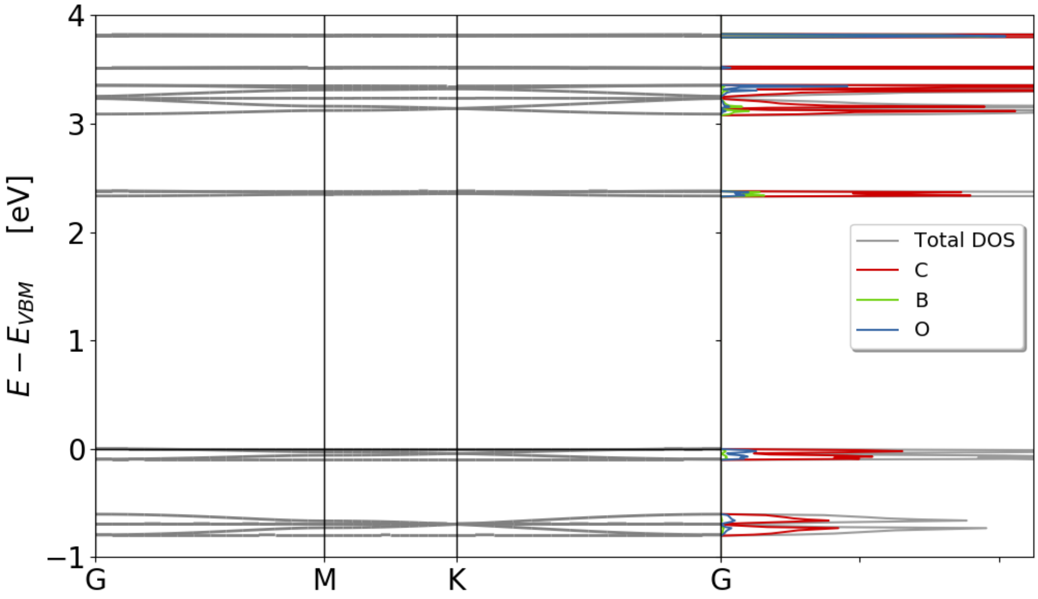

Figure A.5: Band structure and elemental density of states for single layer COF-10. Calculated using the vdW-DF-cx functional.

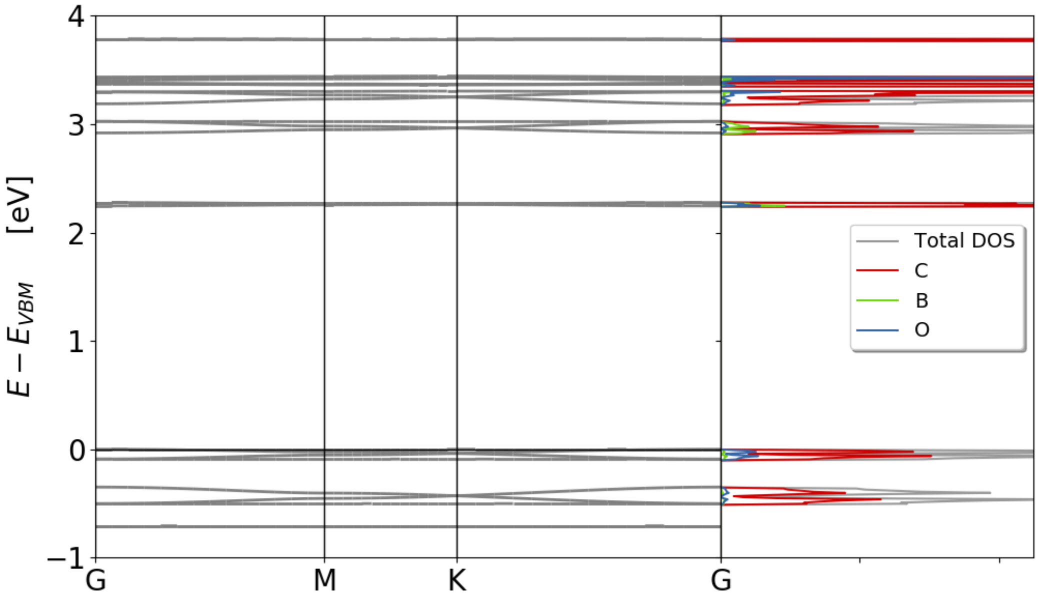

Figure A.6: Band structure and elemental density of states for single layer COF-10. Calculated using the vdW-DF-cx functional.

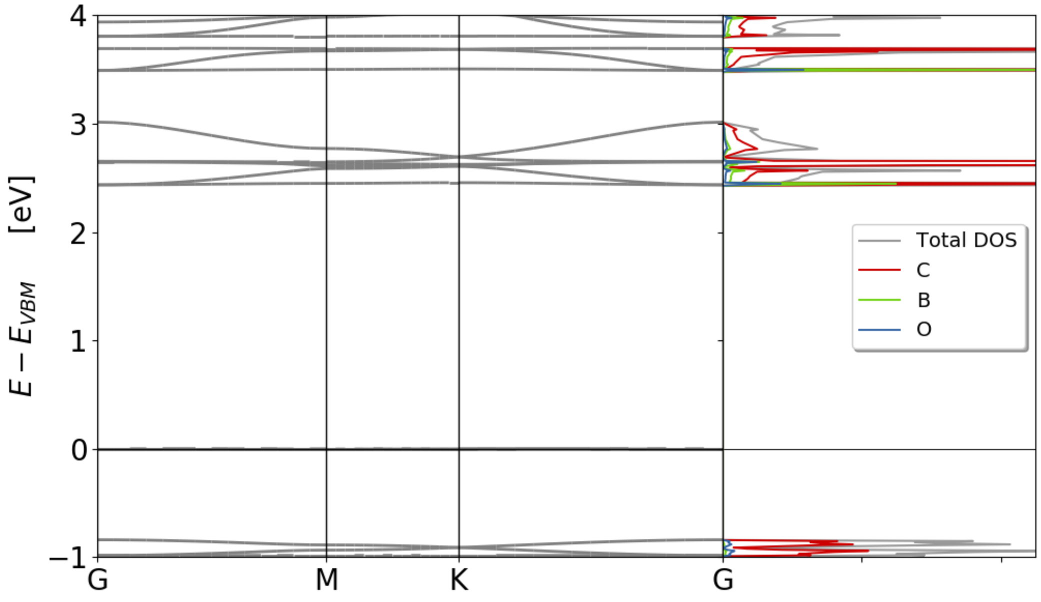

Figure A.7: Band structure and elemental density of states for single layer PPy-COF. Calculated using the vdW-DF-cx functional.

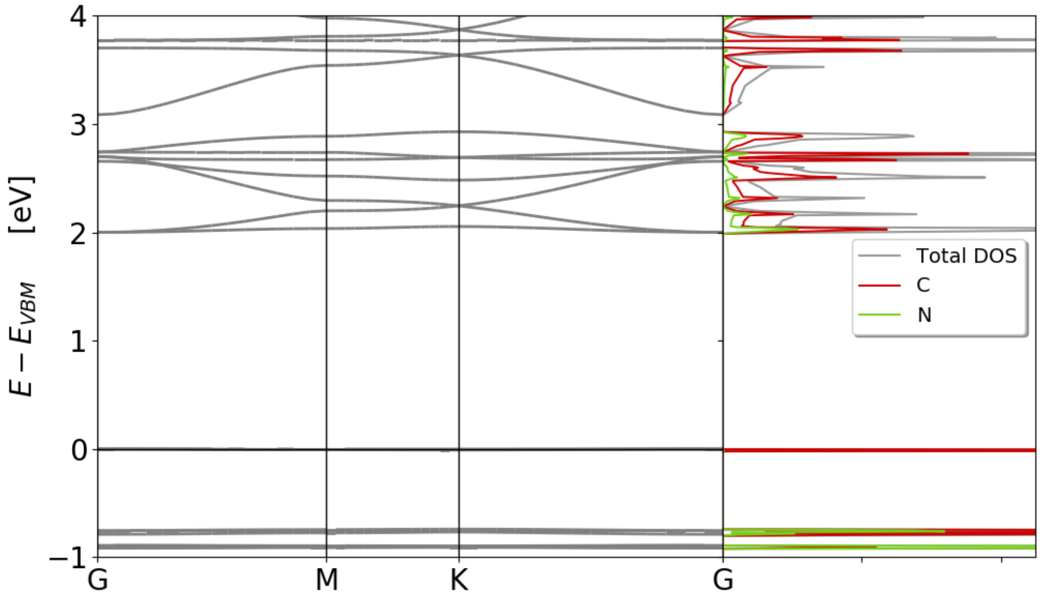

Figure A.8: Band structure and elemental density of states for single layer PPy-CTF. Calculated using the vdW-DF-cx functional.

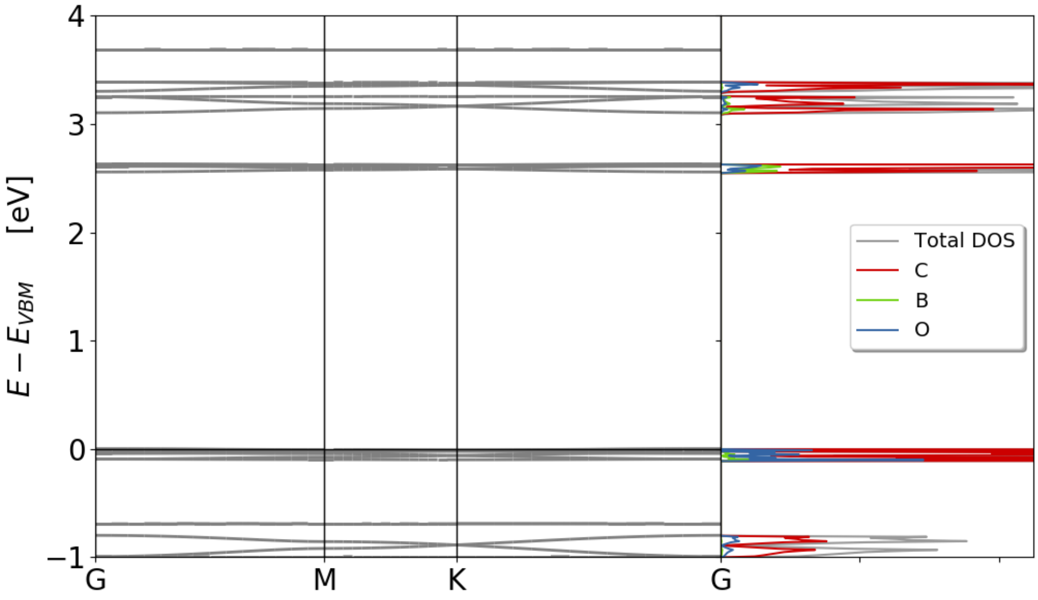

Figure A.9: Band structure and elemental density of states for single layer TP-COF. Calculated using the vdW-DF-cx functional.

A.2 Layered BS and DOS

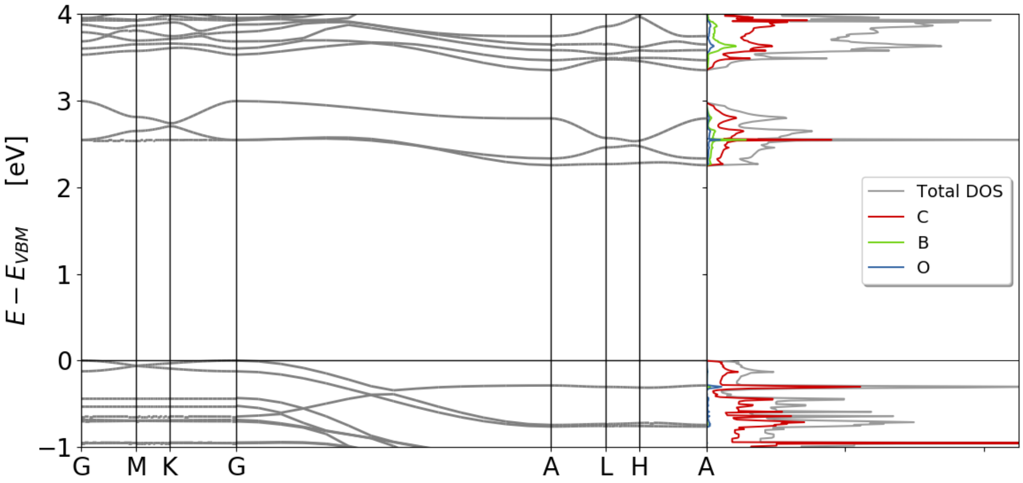

Figure A.10: Band structure and elemental density of states for optimally AA-stacked COF-1X. Calculated using the vdW-DF-cx functional.*

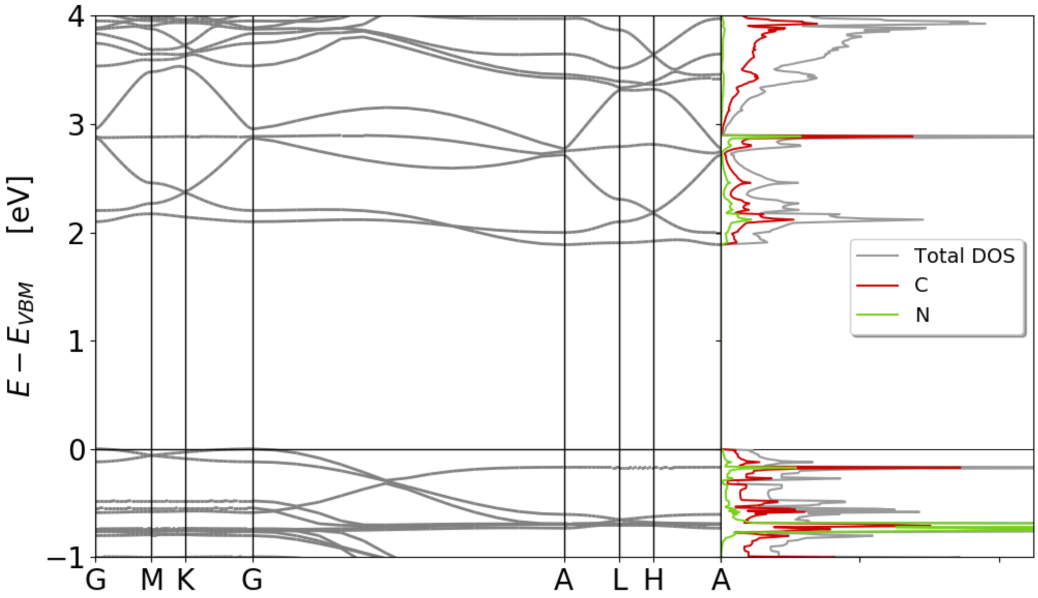

Figure A.11: Band structure and elemental density of states for optimally AA-stacked CTF-1X. Calculated using the vdW-DF-cx functional.*

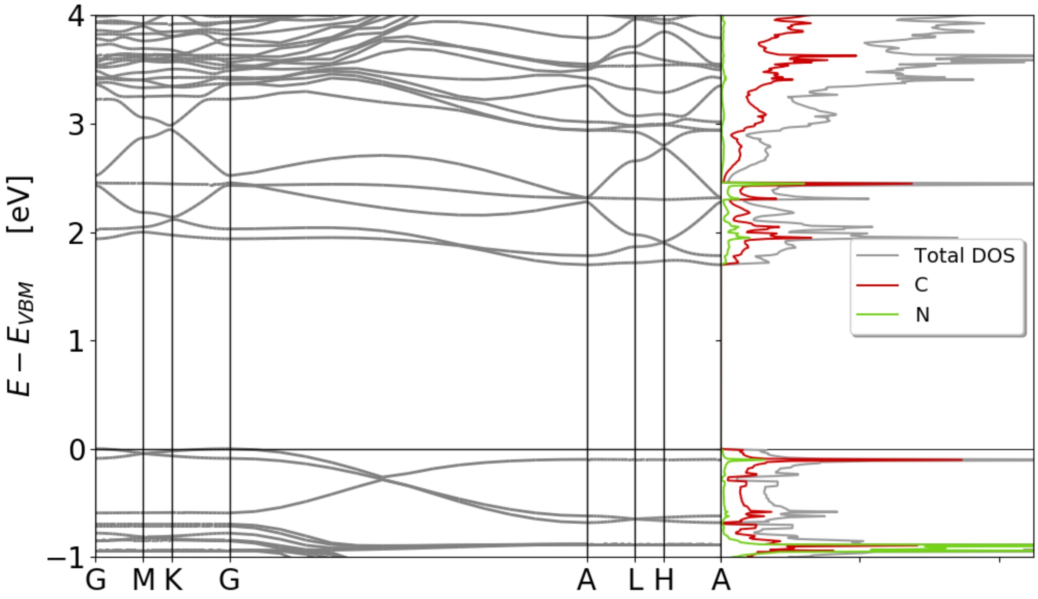

Figure A.12: Band structure and elemental density of states for optimally AA-stacked CTF1Y. Calculated using the vdW-DF-cx functional.*

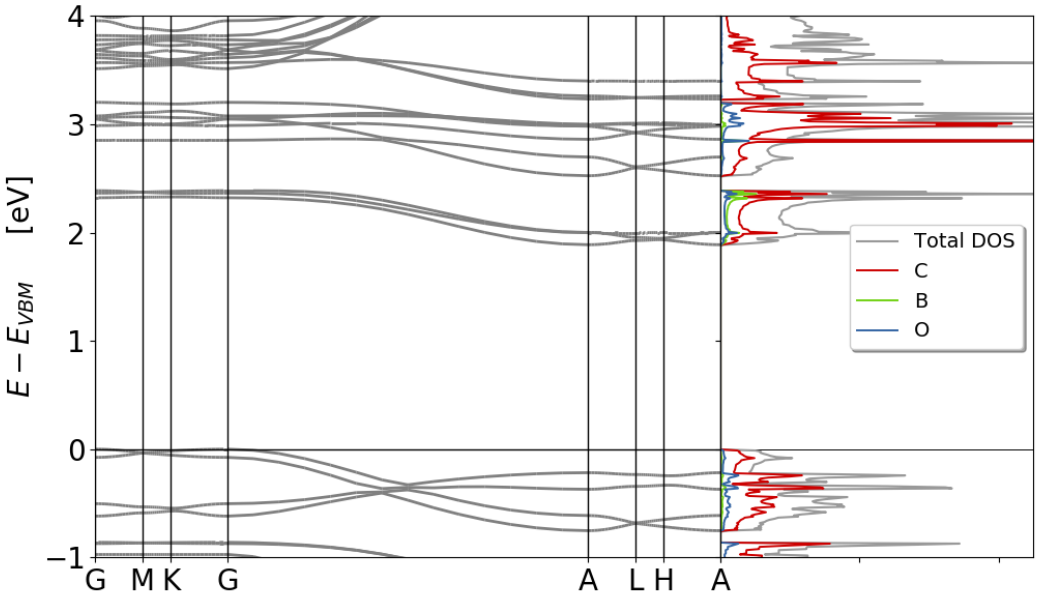

Figure A.13: Band structure and elemental density of states for optimally AA-stacked COF-5. Calculated using the vdW-DF-cx functional.*

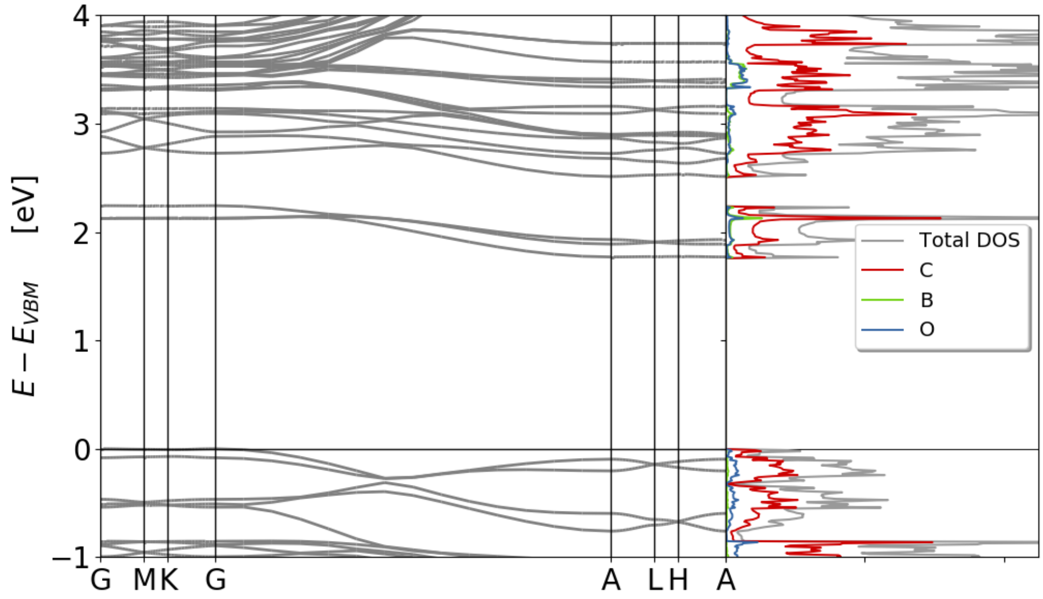

Figure A.14: Band structure and elemental density of states for optimally AA-stacked COF-10. Calculated using the vdW-DF-cx functional.*

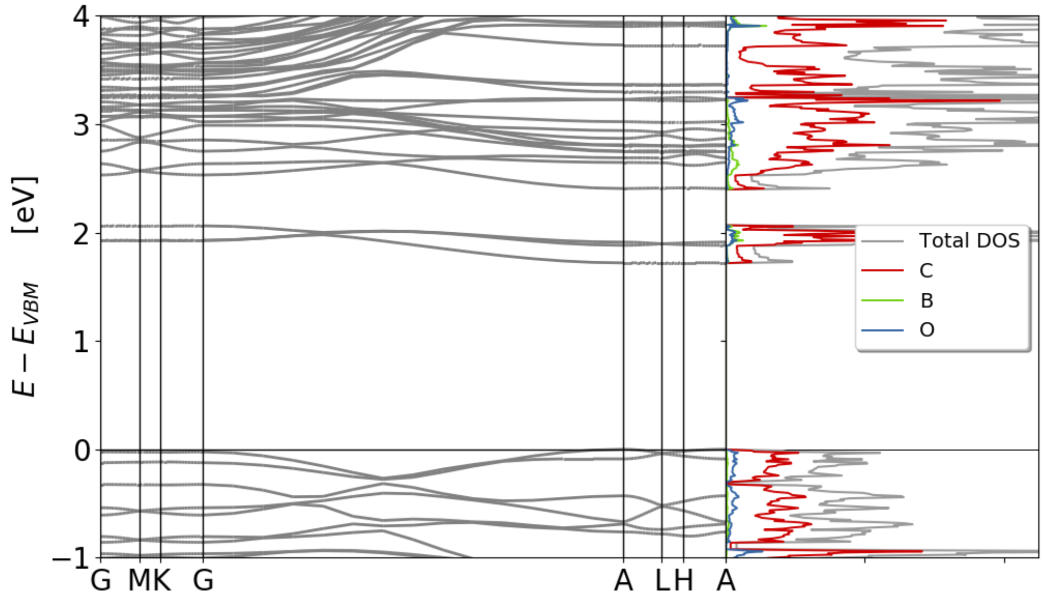

Figure A.15: Band structure and elemental density of states for optimally AA-stacked COF-15. Calculated using the vdW-DF-cx functional.*

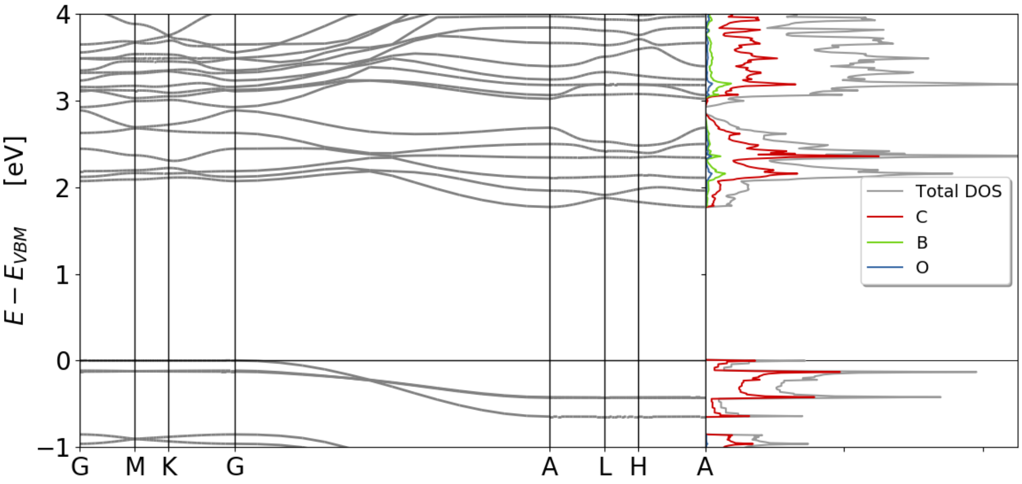

Figure A.16: Band structure and elemental density of states for optimally AA-stacked PPy-COF. Calculated using the vdW-DF-cx functional.*

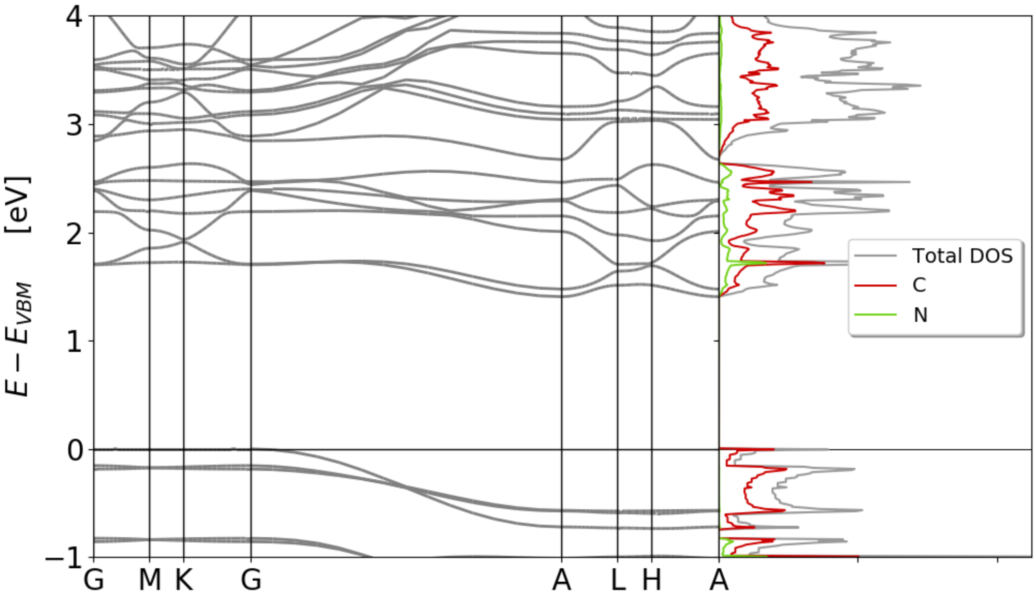

Figure A.17: Band structure and elemental density of states for optimally AA-stacked PPy-CTF. Calculated using the vdW-DF-cx functional.*

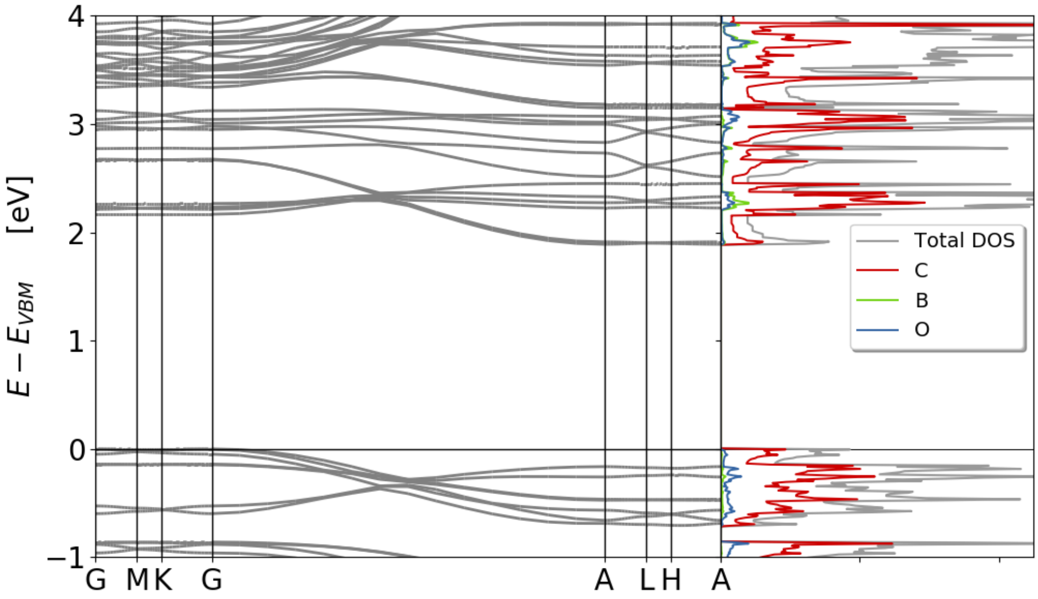

Figure A.18: Band structure and elemental density of states for optimally AA-stacked TP-COF. Calculated using the vdW-DF-cx functional.*

List of Figures

1.1 Illustational picture of a single layer of COF-1. Boron, oxygen, carbon and hydrogen are represented with pink, red, black and white, respectively. Twelve hexagonal boroxide and phenyl rings combine to construct bigger hexagonal pores. The boroxide rings have three fold rotational symmetry and are referred to as nodes while the phenyl rings with two fold rotational symmetry and are referred to as linker. 2

1.2 In the diagram we see the different possible combinations of linkers and nodes that make up our candidate materials. These are not the chemical precursors but just the molecular building units (with dangling bonds) we can imagine combining to form the extended structures. 3

3.1 Illustrated here is one pore of optimally AA*-stacked CTF-1. Every layer is translated a fixed distance 1.82 Å compared to the next along one of the directions parallel to the linker as suggested by the stacking study results. 13

4.1 Band structure and elemental density of states for single layer COF-1. Single layer COF-1 has the largest band gap of all the candidate materials. Calculated using the vdW-DF-cx functional. 18

4.2 Band structure and elemental density of states for single layer CTF-1. The Band gap is lower and the band widths are higher in CTF-1 compared to COF-1. Calculated using the vdW-DF-cx functional. 18

4.3 Band structure and elemental density of states for single layer COF-1Y. COF-1Y has similar features to that of COF-1, expect that all the bands are squeezed together. Calculated using the vdW-DF-cx functional. 19

4.4 The tug of war between the stabilizing vdW-interactions and repulsive forces cause by overlap of orbitals are clearly shown when the total energy of the optimally AA*-stakced COFs are calculated with different interlayer distances. The forces stabilize at a equilibrium distance of 3.34 Å, close to the experimentally reported value of 3.32 Å. [12] 20

4.5 Band structure and elemental density of states for optimally AA*-stacked COF-1. The insert in the band gap illustrate how two layers would stack. We see the dispersion in the bands when going from *Gamma* to A, which corresponds to the out of plane direction in real space. Calculated using the vdW-DF-cx funtional. 21

4.6 Band structure and elemental density of states for optimally AA*-stacked CTF-1. The insert in the band gap illustrate how two layers would stack. Features are still similar to that of COF-1 but the bands are much broader. Calculated using the vdW-DF-cx funtional. 21
4.7 Band structure and elemental density of states for optimally AA*-stacked COF-1Y. The same trends applies when going from COF-1 to COF-1Y for the stacked structures, Bands get pinched when adding extra phenyl-rings to the linkers. Calculated using the vdW-DF-cx funtional. 22
4.8 Cubic interpolation of the AA*-stacking landscape for each COF. The exotic color-scheme is chosen because it finely resolves the upper and lower part of the energy range. 23
4.9 Cubic interpolation of the AA*-stacking landscape for each COF 24
4.10 Cubic interpolation of the AA*-stacking landscape for each COF 25

A.1 Band structure and elemental density of states for single layer COF-1X. Calculated using the vdW-DF-cx functional. 34
A.2 Band structure and elemental density of states for single layer CTF-1X. Calculated using the vdW-DF-cx functional. 34
A.3 Band structure and elemental density of states for single layer CTF-1Y. Calculated using the vdW-DF-cx functional. 35
A.4 Band structure and elemental density of states for single layer COF-5. Calculated using the vdW-DF-cx functional. 35
A.5 Band structure and elemental density of states for single layer COF-10. Calculated using the vdW-DF-cx functional. 36
A.6 Band structure and elemental density of states for single layer COF-10. Calculated using the vdW-DF-cx functional. 36
A.7 Band structure and elemental density of states for single layer PPy-COF. Calculated using the vdW-DF-cx functional. 37
A.8 Band structure and elemental density of states for single layer PPy-CTF. Calculated using the vdW-DF-cx functional. 37
A.9 Band structure and elemental density of states for single layer TP-COF. Calculated using the vdW-DF-cx functional. 38
A.10 Band structure and elemental density of states for optimally AA*-stacked COF-1X. Calculated using the vdW-DF-cx functional. 39
A.11 Band structure and elemental density of states for optimally AA*-stacked CTF-1X. Calculated using the vdW-DF-cx functional. 39
A.12 Band structure and elemental density of states for optimally AA*-stacked CTF1Y. Calculated using the vdW-DF-cx functional. 40
A.13 Band structure and elemental density of states for optimally AA*-stacked COF-5. Calculated using the vdW-DF-cx functional. 40
A.14 Band structure and elemental density of states for optimally AA*-stacked COF-10. Calculated using the vdW-DF-cx functional. 41
A.15 Band structure and elemental density of states for optimally AA*-stacked COF-15. Calculated using the vdW-DF-cx functional. 41

A.16 Band structure and elemental density of states for optimally AA*-stacked PPy-COF. Calculated using the vdW-DF-cx functional. 42
A.17 Band structure and elemental density of states for optimally AA*-stacked PPy-CTF. Calculated using the vdW-DF-cx functional. 42
A.18 Band structure and elemental density of states for optimally AA*-stacked TP-COF. Calculated using the vdW-DF-cx functional. 43

List of Tables

4.1 Unit cell parameters and range of bond lengths for single layer COFs. Calculated with the vdW-DF-cx functional. 16
4.2 Comparison of the band gaps of single layer and stacked structures 19
4.3 Optimal AA*(x,y)-stacking arrangements and interlayer distance. Calculated with the vdW-DF-cx functional. 26